(19) Europäisches Patentamt
European Patent Offic
Offic uropé n des brev ts

(11) Publication number : **0 595 527 A1**

(12) EUROPEAN PATENT APPLICATION

(21) Application number : **93308312.3**

(22) Date of filing : **19.10.93**

(51) Int. Cl.[5] : **H01J 61/44**, C09K 11/72, H01J 61/48

(30) Priority : **19.10.92 US 963873**

(43) Date of publication of application : **04.05.94 Bulletin 94/18**

(84) Designated Contracting States : **BE DE FR GB NL**

(71) Applicant : **FLOWIL INTERNATIONAL LIGHTING (HOLDING) B.V.**
"Atrium" Building 2nd Floor, Strawinskylaan 3037
NL-1077 ZX Amsterdam (NL)

(72) Inventor : **Pappalardo, Romano G.**
131 Pratts Mill Road
Sudbury, MA 01776 (US)

(74) Representative : **Butler, Michael John et al**
FRANK B. DEHN & CO. Imperial House 15-19 Kingsway
London, WC2B 6UZ (GB)

(54) Fluorescent lamps with high color-rendering and high brightness.

(57) A fluorescent lamp having a plurality of lamp phosphors for converting ultraviolet radiation to visible illumination, in which the lamp phosphor comprises a plurality of metameric blends. The metameric blends of lamp phosphors having substantially identical color coordinates. Cheaper phosphor blends may then be used in conjunction with more expensive fluorescent coatings of the same color coordinate to produce a cheaper fluorescent lamp of the same color coordinates.

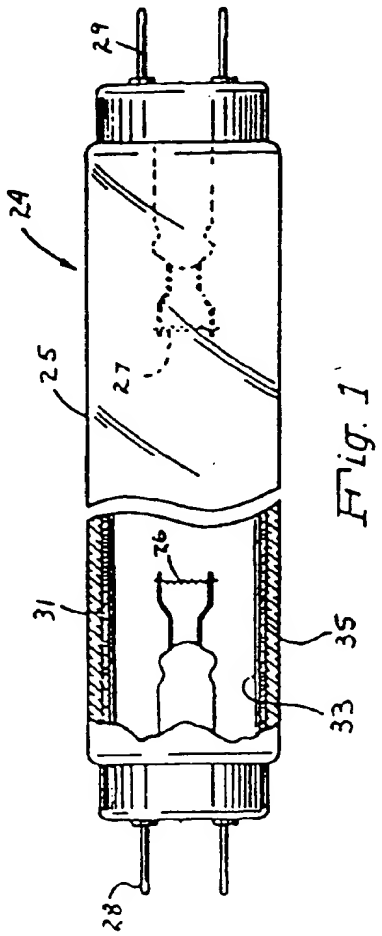

Fig. 1

EP 0 595 527 A1

This invention relates to fluorescent lamps and fluorescent-lamp phosphors. and specifically to improvements in cost/performance of fluorescent lamps as a result of utilizing appropriate combinations of phosphors.

Electrical discharges in a low-pressure noble gas containing mercury generate UV radiation (mainly at 254nm) with high efficiency. This UV radiation from the mercury/noble-gas plasma can be converted into visible light by appropriate materials (phosphors). The combination of this low-pressure plasma plus the phosphor constitutes a fluorescent lamp.

For a given low-pressure plasma, the fluorescent-lamp output depends on the phosphor (or phosphor combination) utilized. In the industry the fluorescent-lamp output is specified radiometrically by its Spectral Power Distribution (SPD). namely by the radiant power per wavelength interval over a spectral region (typically from 375nm to 760nm) that spans not only the visible region, but also a portion of the near UV spectrum and of the near-infrared spectrum.

Regardless of the phosphor(s) used, the SPD from a fluorescent source is intrinsically different from that of a black-body radiator, such as the sun or an incandescent lamp. The basic reason for this is that the output from a fluorescent lamp will always contain the sharp emission lines produced in the visible by the plasma-excited mercury atoms, and these emission lines are absent in incandescent lamps or in natural (sun) light.

With the introduction of the fluorescent lamps, the need arose in the industry to correlate and compare the output properties of these non-blackbody radiators with those of known white emitters, such as incandescent lamps. The basis of this correlation is the lamp SPD. In effect, by mathematically convoluting the SPD with three spectral-response functions (color-matching functions) associated with the human visual perception, one can mathematically extract from the SPD two quantities (x and y) defined as the "chromaticity coordinates" of the fluorescent lamp. Each pair of chromaticity coordinates defines a point in the so-called color plane. In particular, the SPD's from blackbody radiators (incandescent sources) define in the color plane a line called the "planckian locus". All commercial sources for general-illumination purposes are located on, or in the vicinity of. the planckian locus.

A representative spectral convolution involving the SPD will be of the form:

$$\int_a^b SPD(\lambda)\cdot R(\lambda)d\lambda \quad (1)$$

with $R(\lambda)$ one of the spectral-response functions, and with the integration limits being typically a=380nm and b=760nm.

Similarly, a convolution of the SPD with one of the aforementioned response functions[wy1], the luminous-efficiency function V_λ, gives the lumen content of the lamp output, which is a measure of the intensity of the visual stimulus produced by the source in a (typical) human observer. These mathematical transformations have been detailed in various publications[cl1,cl2] of the CIE (Commission Internationale de l'Eclairage).

Two sources, such as a fluorescent lamp and an incandescent lamp, can have different SPD's but the same color coordinates; when viewed directly they produce the same visual perception. In such a case the observer visual response is spectrally averaged over the entire SPD of the source. and this averaging is equivalent to the mathematical convolution that produced the color (or chromaticity) coordinates in the first place. Sources with the same color coordinates, but different SPD are defined as being "metameric".

Problems arise when objects are being observed under illumination by metameric SPD's. In such a case the observer perception is no longer produced by a spectral average over the entire SPD, but only over the source SPD as reflected from the object being viewed. In general, the color (and hence the color coordinates) of a given object will appear different, when viewed under illumination by one or the other of the metameric sources (the fluorescent source and the corresponding incandescent source).

Mathematical procedures were prescribed by the CIE in an attempt to quantify these color differences. The procedures again involve operations on the source SPD, which is now convoluted with the reflectance spectra of eight objects. chosen as representative standards of the range of colors normally encountered. Both the fluorescent-lamp SPD and the SPD of a "temperature correlated" blackbody (incandescent) source are convoluted with the eight reflectance spectra of the standards. In general, the eight quantities derived from the convolution with the fluorescent-source SPD will differ from the corresponding set of eight values obtained with the blackbody SPD. These differences lead to a distortion in color perception, or color rendering, associated with the fluorescent source. The CIE prescribes further mathematical processing of these differences, to arrive at a final set of eight color-rendering indices R_a (with a=1,2,..8). In practice the industry relies on an single, overall figure-of-merit for the color rendering, namely the general color-rendering index or CRI, which results from a weighed average of the individual R_a. By definition, CRI=100 for a black-body (incandescent) source.

Since the SPD of an incandescent source varies smoothly over the visible spectral region, while that of a fluorescent lamp has sharp discontinuities at the sp ctral location of the Hg lines, in order to maximize the CRI of a fluorescent source one can state, as a rule-of-thumb, that the output from the fluorescent source must by distributed over the visible spectral region in a fairly uniform fashion. Then the spectral averages over

various s ctions of the visible spectrum will not markedly differ from the analogous spectral averages for an incandescent source. But there are no specific rules on how to perform this optimization of the CRI. In any case the CRI of the fluorescent source will be a very sensitivity function of the spectral profile of the SPD.

In summary, the output from a fluorescent lamp is fully characterized by its SPD. From the latter one can mathematically derive: its color coordinates, which are roughly speaking a measure of the source "whiteness"; the lumen output (brightness); and the source CRI, namely its ability to faithfully reproduce colors. For a fluorescent source with a given color-point, ideally one would like to simultaneously maximize brightness and CRI, but this is intrinsically impossible. In practice, one strives, by the choice of appropriate phosphor combinations (blends), to produce lamps whose output provides simultaneously high values of the CRI and of the lumen output. In the choice of phosphor-blend components considerations of phosphor cost cannot be ignored, since classes of fluorescent-lamp phosphors currently in use incorporate rare-earth elements, which are very expensive.

Since the lamp output-characteristics are completely described by the lamp SPD, the process of optimizing the lumen output/CRI combination by means of phosphor blending can be carried out theoretically at first, without actually having to build lamps, as long as we have available a mathematical technique to construct SPD's that meet some specific performance objectives. The building blocks ("component" SPD's) for this process are here conveniently chosen as the SPD's of lamps containing a single phosphor.

In accordance with the present invention, there is provided a fluorescent lamp comprising a plurality of metameric blends of lamp phosphors for converting ultraviolet radiation to visible illumination.

The present describes a subset of the SPD-optimization process, in the sense of concentrating on the search of total (lamp) SPD's exhibiting high levels of lumen output and high CRI values, in the neighborhood of eighty, for 40Watt-T12 fluorescent sources with color coordinates of :

$$x = 0.387;\ y = 0.391 \quad (2)$$

Such sources approximate the output of an incandescent source at about 4,000K (more exactly at about 3,950K), and are produced by GTE Products Corp. under the trade name of "Lite-White Deluxe" (LWX) lamps. The methodology to be discussed is applicable in all generality to sources whose color point falls on the planckian locus, or in its vicinity, but here only the results for about 4,000K sources will be reported.

Embodiments of the present invention will now be described by way of example only, and with reference to the accompanying drawings, in which:

FIG. 1 is perspective view partially broken away of a low pressure mercury discharge fluorescent lamp construction utilizing a dual layer phosphor coating.

FIG. S1 shows the SPD after 100 hours of operation for a 40Watt-T12 lamp containing Sylvania phosphor type #2194.

FIG. S2 shows the SPD after 100 hours of operation for a 40Watt-T12 lamp containing Sylvania phosphor type #2288.

FIG. S3 shows the SPD after 100 hours of operation for a 40Watt-T12 lamp containing Sylvania phosphor type #2293.

FIG. S4 shows the SPD after 100 hours of operation for a 40Watt-T12 lamp containing Sylvania phosphor type #2345.

FIG. S5 shows the SPD after 100 hours of operation for a 40Watt-T12 lamp containing Sylvania phosphor type #246.

FIG. S6 shows the SPD after 100 hours of operation for a 40Watt-T12 lamp containing Sylvania phosphor type #290,

FIG. S7 shows the SPD after 100 hours of operation for a 40Watt-T12 lamp containing Sylvania phosphor type #4300.

FIG. S8 shows the SPD after 100 hours of operation for a 40Watt-T12 lamp containing Sylvania phosphor type #4381.

FIG. S9 shows the SPD after 100 hours of operation for a 40Watt-T12 lamp containing Sylvania phosphor type #4459.

FIG. S10 shows the SPD associated with the Gd pentaborate:Ce;Mn phosphor, after 100 hours of operation in a 40Watt-T12.

FIG. hb1 shows the SPD for the halo blend at the LWX color point (x=0.387; y=0.391), with the composition and output properties indicated in the body of the Figure.

FIG. i0 shows lumen and CRI characteristics of quad blend containing phosphor types #246, #2194, #2293, and #2345 as a function of the fractional content in the #2194 phosphor. Blends for the LWX color point (x=0.387; y=0.391).

FIG. i1 shows the SPD for a quad blend for the LWX color point and containing phosphors #246, #2194, #2293, and #2345. Mixing coefficients and output characteristics are also indicated. No halo addition.

FIG. i2 shows the effect of metameric mixing on the CRI and lumen output for a tri-blend for the LWX color point, and based on phosphors #246, #2293, and #2345, according to the c_i mixing coefficients listed in the Figure.

FIG. i3 shows the increased CRI resulting from metameric mixing for a specific LWX quad-blend based on phosphors #246, #2194, #2293, and #2345, according to the c_i mixing coefficients listed in the Figure.

FIG. i4 shows the increase in CRI and lumen output resulting from metameric mixing for a specific LWX quad-blend based on phosphors #246, #2194, #2293, and #2345, according to the c_i mixing coefficients listed in the Figure. The CRI reaches the value of 90 at 30% halo admixing.

FIG. ii1 shows the increased CRI resulting from metameric mixing for a specific LWX quad-blend based on phosphors #246, #2194, #2288, and #2345, according to the c_i mixing coefficients listed in the Figure.

FIG. ii2 shows the increase in CRI and lumen output resulting from metameric mixing for a specific LWX tri-blend based on phosphors #246, #2194, and #2345, according to the c_i mixing coefficients listed in the Figure. The CRI exceeds 90 at 45% halo admixing.

FIG. iii1 shows the increased CRI resulting from metameric mixing for a specific LWX quad-blend based on phosphors #246, #2288, #2345, and #290, according to the c_i mixing coefficients listed in the Figure.

FIG. fl1 shows the lumen and CRI characteristics of quad blend containing phosphor types #246, #2194, #2288, and L93S as a function of the fractional content in the #2194 phosphor. Blends for the LWX color point (x=0.387; y=0.391).

FIG. fl2 shows the increase in CRI and lumen output resulting from metameric mixing for a specific LWX tri-blend based on phosphors #246, #2194, #2284, and L93S, according to the c_i mixing coefficients listed in the Figure. The CRI exceeds 90 for halo fractions ranging from 0.25 to 0.40.

FIG. dr1 shows the SPD of a LWX metameric mix based on a tri-blend containing phosphors #246, #2194, and #2345. Mix of 0.45 halo blend and 0.55 quad blend. CRI at 90.4 and about 3045 lumens.

FIG. le1 shows the SPD of the experimental lamp with the tri-blend containing phosphor types #246, #2194, and #2345.

FIG. le2 shows the SPD of the experimental lamp with the halophosphate blends.

FIG. le3 shows the SPD of the experimental lamp containing the metameric mix of 45% halophosphate phosphor, as per Figure le2, and 55% of the triblend of Figure le1.

FIG. bl1 shows a portion of the planckian locus and location of the color points of the test lamps. Legend: halo, halophosphate-containing lamp of Figure le2; tri is the tri-blend of Figure le1; MM is the lamp with the metameric mix of Figure le3. The remaining color points are for sources at 3000K. 2500K and 2000K.

Referring to FIG. 1, there is shown a fluorescent lamp 24 containing a phosphor excitable to fluorescence. The lamp 24 comprises a tubular, hermetically sealed, glass envelope 25. Electrodes 26 and 27 are sealed in the ends of envelope 25. Suitable terminals 28 and 29 are connected to the electrodes 26 and 27 and project from envelope 25. The electrodes 26 and 27 extend through glass presses in mount stems to the terminals 28 and 29.

The interior of the tube is filled with an inert gas such as argon or a mixture of argon and krypton at a low pressure, for example 2 torr, and a small quantity of mercury, at least enough to provide a low vapor pressure during operation. An arc generating and sustaining medium such as one or more inert gases and mercury is included within envelope 25 so that ultraviolet radiation is produced in the interior of the glass envelope during lamp operation. A phosphor coating 31 on the interior surface of the glass envelope converts the emitted ultraviolet radiation to visible illumination having a white color.

In accordance with the principles of the present invention, an improved phosphor layer of the present invention which is illustrated at 33 comprises a plurality of metameric blends of lamp phosphors for converting ultraviolet radiation to visible illumination. Although dual layers of metameric phosphor blends are shown in FIG. 1, a single layer comprising a mixture of metameric phosphor blends may be utilized as a single coat.

When a dual layer is utilized as shown in FIG. 1, the first layer 35 is deposited on the inner glass surface and a second phosphor layer or top layer 33 is deposited on the first phosphor layer 35. The use of a dual phosphor layer permits the weight of phosphor utilized in the second or top coat to be reduced and a less expensive phosphor to be utilized as the first layer 35. The first layer 35 preferably comprises a finely divided metameric blend of fluorescent calcium haloapatite phosphor exhibiting the desired white color point. The second layer or top layer 33 comprises a metameric quad phosphor blend on the inside of the tube so that a substantial portion of the ultraviolet radiation is converted to visible illumination having a white color. The amount of the metameric quad-phosphor blend applied is generally between about 10 percent and 50 percent of the total combined phosphor weight of the total of the metameric quad-blend and the metameric halophosphor.

The derivation to be detailed next goes through the following stages.

* First, various combinations of four primary (component) SPD's are systematically explored to identify total (lamp) SPD's exhibiting a target color-point and the required levels of CRI and lumen output.

- Second, it is shown how the CRI values can be raised by combining two m tameric blend-SPD's with the same target color-point, but individually exhibiting a relatively-low CRI.
- Third, guidelines for implementation in actual lamps are described.
- Fourth, examples of reduction to practice are reported.

1. SPD of four-component (quad) blends.

The main focus of the present treatment is on the results of combining four SPD's, or equivalently, on blending four phosphors. There is a compelling reason for considering four-component blends. When three component SPD's are combined to obtain a total SPD with a pre-assigned target color-point, namely

$$SPD_{(tot)} = \Sigma_i \, c_i \cdot (SPD)_i \quad (3)$$

with C_i=1, 2, 3,
and

$$\Sigma_i \, c_i = 1 \quad (4)$$

either no solution is possible, or there is a unique solution for the c_1, c_2, and c_3 mixing coefficients. This produces one single value for the CRI and for the lumen output from the blend. The solution exists whenever the target color-point is contained within the triangle formed by the color-points of the three blend components.

As a concrete example, suppose a halophosphate blend with the color point of eq. 2. is required. Such a blend can be obtained for instance by combining the SPD's of the halophosphate phosphor types #4381, #4459. and #4300 listed in Tables b1 and b2. The resulting SPD of the LWX halo-blend will be produced by the combination:

$$0.120 \cdot SPD(\#4381) + 0.796 \cdot SPD(\#4459) + 0.084 \cdot SPD(\#4300) \quad (5)$$

where by SPD(#4381) we mean the 100hrs-SPD pertaining to a (performance optimized) 40Watt-T12 lamp containing only phosphor #4381, and so forth for SPD(#4459) and SPD(#4300). The c_i mixing coefficients of eq. 3 therefore assume the values: 0.120; 0.796; and 0.084, respectively.

On the other hand, if four primary SPD's are combined (four-component phosphor blend) an infinity of solutions satisfy eqs (3) and (4), with as many sets of c_1, c_2, c_3, and c_4 mixing coefficients. To each solution there will correspond a pair of values for the CRI and the lumens, and so an infinite set of CRI and lumen values is accessible for selection.

The detailed composition of this infinite set of four-component (quad) blends can be sampled by a process of mathematical induction, starting from the mixing of binary blends with ternary blends. Proprietary computer software was developed to systematically explore the range of existing solutions (c_i mixing coefficients) and to sequentially derive the lumen content and CRI of the various $SPD_{(tot)}$ of eq. 3.

In this application we are not mainly concerned with the details of the mathematical derivation, but rather with the actual SPD's obtained, on the basis of the "primary" or "component" SPD's of lamps containing the phosphors listed in Table b1. A summary listing of the relevant phosphor emission-color, powder weight in lamps, and output characteristics at 100 hours of operation is given in Table b2 for 40Watt-T12 lamps containing a single phosphor. The actual SPD's are shown in detail in Figures s1 to s10. In turn, the SPD of the LWX halo-blend as derived from eq. 5 is given in Figure hb1.

Table b1. Approximate chemical composition of Sylvania phosphors considered in the present application

Phosphor type (Sylvania™)	Composition
#2194	BaMgAluminate:Eu;Mn
#2288	Zinc ortho-silicate:Mn
#2293	(Ce,Tb)Mg Hexa-aluminate
#2345	Yttrium Oxide:Eu
#246	BaMg Aluminate:Eu
#290	Ca Silicate:Pb;Mn
#4300	Ca apatite:Sb;Mn (halo-phosphate)
#4381	Ca fluoroapatite:Sb;Mn (halo-phosphate)
#4459	Ca apatite:Sb;Mn (halo-phosphate)
(L93S)*	Gd pentaborate:Ce;Mn

* not an actual Sylvania phosphor, but "ad-hoc" designation for a specific lamp-SPD.

Table b2 Composition, powder weight, and output characteristics (at 100 hours of operation) of single-component W40-T12 lamps utilized in the derivation.

Phos. type (Sylvania)	Emiss. color	Rare-earth*	weight (grams)	lumen at 100hrs	color coordinates x	y
#246	blue	yes	5.2	1,006	0.151	0.088
#2194	green	yes	5.9	3,467	0.162	0.560
#2288	green	no	6.0	4,900	0.247	0.635
#2293	green	yes	6.6	4,732	0.315	0.554
#290	red	no	3.1	1,900	0.589	0.331
#2345	red	yes	6.1	2,750	0.506	0.377
#4300	white	no	7.6	3,260	0.440	0.406
#4381	yellow	no	6.3	3,410	0.406	0.430
#4459	white	no	6.3	3,100	0.379	0.384
(L93S)	red	yes	n/a	1,795	0.526	0.309

* The presence of rare-earth elements in a phosphor typically makes it 50 times more expensive than such halophosphate phosphors as #4300, #4381, and #4459.

Although quad blends can be obtained by taking all possible combination of existing lamp phosphors, only five such combinations of four phosphors will be described here, namely:

1. The addition of phosphor #2194 (see Tables b1 and b2) to a typical "tri-color" blend (i.e., phosphors #246, #2293, #2345) currently used in the industry for high-CRI, high-efficacy[ve1] fluorescent lamps.
2. Same as above, but with #2293 replaced by #2288 (see Tables b1 and b2).
3. Phosphors #246 and #2288, plus the two red-emitting phosphors #2345 (line emitter) and #290 (band emitter). See Tables b1 and b2.
4. Phosphor #246, the two green-emitting phosphors #2194 and #2288, and red-emitting Gd pentaborate: Ce;Mn (see Tables b1 and b2).
5. Blue-emitting #246, green-emitting #2194, and the two red-emitters #2345 and #290.

In all five cases listed above, after determining the output characteristics of the quad blends, the metameric mixing of the quad blends with the LWX halo-blend of eq. 5 was also explored.

Since two metameric SPD's combine to produce a total SPD with the same color point, metameric SPD's can be mixed in any arbitrary proportion, and still maintain some pre-assigned color coordinates. In what follows "metameric mixing" will m an specitically the admixing of a LWX quad-blend with the LWX halo-blend of eq. 5.

In view of the low cost of the halophosphate phosphors, economic advantages will always result from this "metameric mixing". Furthermore, in the most favorable cases the CRI, brightness and cost of th final LWX-mix will all be improved by the addition of the halophosphate phosphors.

1. Blends of #246; #2194; #2293, #2345.

A representative sampling of the infinite set of possible formulations, with the respective values of lumen output and CRI, are listed in Table p1. The entries in the columns labelled by the phosphor types correspond to the mixing coefficient c_i of eqs. 3 and 4. The output characteristics are also plotted in Figure i0 as a function of the fractional content in #2194.

From inspection of Table p1 and Figure i0 it can be concluded that the addition of #2194 to the tri-color blend of #246, #2293, and #2345 (first row of Table p1, and leftmost data points in Figure i0) produces a broad increase in the CRI, to a peak value of ~87.1 for 0,115·SPD(#2194). The SPD of this blend is shown in Figure i1, and is listed in detail in Appendix 1.

The CRI of the quad blend exceeds that of the original tri-blend for #2194 fractions ranging from 0 to ~0.30 (Figure i0 and Table p1). Then the CRI drops as the #2194 content is further raised beyond ~0.30. Conversely, the quad-blend lumen output drops linearly as the #2194 content increases (Figure i0).

Moving next to metameric mixes, quite generally the changes in CRI resulting from the admixing of the LWX halo-blend depend on the specific #2194 content in the quad blend. When the #2194 content is zero (first row in Table p1) the quad blend reduces to a triphosphor blend of the type currently employed in the industry. In this case the effect of metameric mixing with the LWX halo-blend of eq. 5 is summarized in Table p2 and Figure i2, where the LWX halo-blend is added in 5% increments, starting at the 10% level, up to a value of 50%.

As the LWX halo-blend is added to the tri-component blend, both the CRI and the lumen output drop monotonically (Figure i2), the latter in a linear fashion, the former in a shallow, parabolic fashion, down to the limiting value of CR1=58.8, which is the CRI for the LWX halo-blend alone (Table p2). The only motivation for adding the LWX haloblend then would be to capitalize on its lower cost, even if lumens and CRI have to be sacrified, compared to the starting tri-component blend.

Table p1. Quad blends for the LWX color-point (x=0.387 and y=0.391), based on phosphors #246, #2194, #2293, and #2345. Composition and predicted output in order of increasing #2194.

Quad-blend content as fractional SPD(#XXXX)				Lumens	CRI
#246	#2194	#2293	#2345		
0.134	0.000	0.476	0.389	3460.3	83.13
0.125	0.061	0.411	0.401	3392.0	85.74
0.117	0.115	0.355	0.412	3333.1	87.09
0.104	0.201	0.264	0.430	3237.1	86.89
0.101	0.220	0.244	0.433	3216.2	86.11
0.097	0.250	0.213	0.434	3182.7	84.76
0.087	0.313	0.146	0.452	3112.0	81.76
0.085	0.324	0.135	0.455	3100.8	81.22
0.084	0.333	0.125	0.456	3091.0	80.77
0.075	0.390	0.065	0.468	3027.0	77.67
0.074	0.398	0.056	0.470	3017.9	77.21
0.066	0.452	0.000	0.481	2958.3	73.82

Table p2. Effect of adding the LWX halo-blend to LWX quad-blends.

QUAD blend: 0.134 (#246); 0.000 (#2194); 0.476 (#2293); 0.389 (#2345)
LWX halo-blend: 0.120 (#4381); 0.796 (#4459); 0.084 (#4300).

Halo fraction	Quad fraction	Lumens	CRI
0.00	1.00	3460.3	83.13
0.10	0.90	3429.4	81.45
0.15	0.85	3413.9	80.47
0.20	0.80	3398.4	79.43
0.25	0.75	3382.9	78.35
0.30	0.70	3367.4	77.24
0.35	0.65	3351.9	76.10
0.40	0.60	3336.5	74.93
0.45	0.55	3321.0	73.74
0.50	0.50	3305.0	72.52
1.00	0.00	3150.6	58.83

A similar trend is observed in the metameric mixing of the quad blend containing 0.061· SPD(#2194), and whose composition is given in the second row of Table p1. The halo addition (Table p3) improves neither the lumen output nor the CRI of the starting quad-blend.

As the #2194 content increases, though, the halo addition is definitely beneficial. This is shown in Figure i3 and in Table p4 for a blend containing 0.220·SPD(#2194). A peak CRI value of ~89 (Table p4) is predicted at a 20% admix of the LWX halo-blend. The lumen loss caused by the halo addition is minimal, only ~13 lumens, that is about one-third of a percent.

It was already mentioned that, as #2194 replaces the more expensive #2293 phosphor, the blend brightness progressively drops (Table p1). When the quad blend reaches a lower brightness than that of the halo-blend, the metameric mixing is instrumental in increasing both brightness and CRI This is shown in Table p5 and in Figure i4 for the quad blend with 0.313 fractional content in #2194. The lumen output increases linearly with the halo-blend content, while the CRI reaches a peak value of ~90 at a 30-35% halo admix.

The metameric mixing was investigated for all the quad blends of Table p1. For the sake of brevity, rather than reproducing for all the blends of Table p1 the detailed results of the metameric mixing, as shown in detail in Tables p2 to p5, we shall explicitly list in Table p6 only those metameric mixes with maximum values of the CRI. Therefore, Table p6 is to be viewed as an expanded version of Table p1. When the metameric mixing increases the CRI of the corresponding quad blend, the halo fraction that produces the highest CRI value is listed below the corresponding quad blend. Values of the CRI in the neighborhood of 90 at lumen levels exceeding 3,000 lumens are achievable with most of the metameric mixes. This is important in countri s wher the building codes require CRI values of 90 for office buildings.

Table p3. Effect of adding the LWX halo-blend to LWX quad-blends.

QUAD blend: 0.125 (#246); 0.061 (#2194); 0.411 (#2293); 0.401 (#2345)
LWX halo-blend: 0.120 (#4381); 0.796 (#4459); 0.084 (#4300).

Halo fraction	Quad fraction	Lumens	CRI
0.00	1.00	3392.0	85.74
0.10	0.90	3367.9	84.98
0.15	0.85	3355.8	84.01
0.20	0.80	3343.7	82.86
0.25	0.75	3331.7	81.63
0.30	0.70	3319.6	80.34
0.35	0.65	3307.5	79.00
0.40	0.60	3295.5	77.62
0.45	0.55	3283.4	76.21
0.50	0.50	3271.3	74.77
1.00	0.00	3150.6	58.83

Table p4. Effect of adding the LWX halo-blend to LWX quad-blends.

QUAD blend: 0.101 (#246); 0.220 (#2194); 0.244 (#2293); 0.433 (#2345)
LWX halo-blend: 0.120 (#4381); 0.796 (#4459); 0.084 (#4300).

Halo fraction	Quad fraction	Lumens	CRI
0.00	1.00	3216.2	86.11
0.10	0.90	3209.7	88.47
0.15	0.85	3206.4	88.84
0.20	0.80	3203.1	88.92
0.25	0.75	3199.8	88.68
0.30	0.70	3196.6	87.78
0.35	0.65	3193.3	86.28
0.40	0.60	3190.0	84.55
0.45	0.55	3186.7	82.67
0.50	0.50	3183.4	80.69
1.00	0.00	3150.6	58.83

Table p5. Effect of adding the LWX halo-blend to LWX quad-blends.

QUAD blend: 0.087 (#246); 0.313 (#2194); 0.146 (#2293); 0.452 (#2345)
LWX halo-blend: 0.120 (#4381); 0.796 (#4459); 0.084 (#4300).

Halo fraction	Quad fraction	Lumens	CRI
0.00	1.00	3112.6	81.76
0.10	0.90	3116.4	85.23
0.15	0.85	3118.3	86.84
0.20	0.80	3120.2	88.31
0.25	0.75	3122.1	89.37
0.30	0.70	3124.0	89.97
0.35	0.65	3125.9	89.65
0.40	0.60	3127.8	88.20
0.45	0.55	3129.7	86.32
0.50	0.50	3131.6	84.17
1.00	0.00	3150.6	58.83

Table p6. Maximum CRI obtainable from metameric mixes of quad blends based on #246, #2194, #2293, and #2345. Comparison with no halo addition. Quad blends listed in order of increasing #2194 content. LWX color point. Part 1.

Quad-blend content as fractional SPD(#XXXX)				Halo fract.	Lumens	CRI
#246	#2194	#2293	#2345			
0.134	0.000	0.476	0.389	0.00	3460.3	83.13
0.125	0.061	0.411	0.401	0.00	3392.0	85.74
0.117	0.115	0.355	0.412	0.00	3333.1	87.09
0.104	0.201	0.264	0.430	0.00	3237.1	86.89
0.104	0.201	0.264	0.430	0.15	3224.1	88.7
0.101	0.220	0.244	0.433	0.00	3216.2	86.11
0.101	0.220	0.244	0.433	0.20	3203.1	88.9
0.097	0.250	0.213	0.434	0.00	3182.7	84.76
0.097	0.250	0.213	0.434	0.25	3174.7	89.3
0.087	0.313	0.146	0.452	0.00	3112	81.76
0.087	0.313	0.146	0.452	0.30	3124.0	90.0

Table p6. Maximum CRI obtainable from metameric mixes of quad blends based on #246, #2194, #2293, and #2345. Comparison with no halo addition. Quad blends listed in order of increasing #2194 content. LWX color point. Part 2.

Quad-blend content as fractional SPD(#XXXX)				Halo fract.	Lumens	CRI
#246	#2194	#2293	#2345			
0.085	0.324	0.135	0.455	0.00	3100.8	81.22
0.085	0.324	0.135	0.455	0.30	3115.7	90.0
0.084	0.333	0.125	0.456	0.00	3091.0	80.77
0.084	0.333	0.125	0.456	0.35	3111.9	90.0
0.075	0.309	0.065	0.468	0.00	3027.0	77.67
0.075	0.309	0.065	0.468	0.40	3076.0	90.4
0.074	0.398	0.056	0.470	0.00	3017.9	77.21
0.074	0.398	0.056	0.470	0.40	3071.0	90.5
0.066	0.452	0.000	0.481	0.00	2958.3	73.82
0.066	0.452	0.000	0.481	0.45	30.44.9	90.4

2 Blends of #246; #2194; #2288, #2345.

The quad blend considered previously contained the rare-earth-activated, green-emitting phosphor #2293. In the set of blends to be discussed next #2293 is replaced by the #2288 phosphor, which does not contain any rare-earth elements and is therefore cheaper. After the derivation of the output characteristics of such blends, the effect of metameric mixing is considered.

A summary listing of the resulting formulations of highest CRI is given in Table s1. The latter is analogous to Table p6, but for the new choice of phosphor types.

There are two limiting cas s of Table s1, whereby the quad blends degenerate into tri-component blends (tri-blends), namely the target color-point can be reached with no #2194 present (first two rows), or with no #2288 present (last two rows). These two cases deserve an explicit treatment. The pertinent results ar summarized in Table s2 and Figure ii1 for the tri-blend based on #246, #2288, and #2345, and in Table s3 and Figur ii2 for the one based on #246, #2194, and #2345.

In the case of the tri-blend with #246, #2288, and #2345 (Table s2 and Figure ii1) the halo addition produces an increase in CRI for halo fractions c_{halo} in the range $O<c_{halo}\leqq 0.4$, up to a peak value of 87.8 for $c_{halo}=0.20$. This entails a modest lumen loss of ~37 lumens, that is ~1% by comparison with the starting tri-blend.

The lumen output of the tri-blend with #246, #2194, and #2345 (~2,960 lumens) is lower (Table s1, Part 2) than that of the LWX halo-blend. Therefore the metameric mixing produces an increase in brightness. Simultaneously, the CRI rises over a broad range of halo fractions (Table s3 and Figure ii2). The remarkably-high CRI and lumen values (CRI>90; lumens in excess of 3,000) should be noted for the metameric mix with 45% halo (Table s3 and Figure ii2). In view of the high halo content, this type of blend will also be quite inexpensive.

Table s1. Maximum CRI obtainable from metameric mixes of quad blends based on #246, #2194, #2288, and #2345. Comparison with no halo addition. Quad blends listed in order of increasing #2194 content. LWX color point. Part 1.

Quad-blend content as fractional SPD(#XXXX)				Halo fract.	Lumens	CRI
#246	#2194	#2288	#2345			
0.140	0.000	0.386	0.473	0.00	3336.2	85.4
0.140	0.000	0.386	0.473	0.20	3299.1	87.8
0.128	0.070	0.326	0.474	0.00	3277.8	84.3
0.128	0.070	0.326	0.474	0.25	3246.0	88.5
0.117	0.140	0.267	0.475	0.00	3219	82.7
0.117	0.140	0.267	0.475	0.25	3202.2	89.0
0.116	0.148	0.260	0.475	0.00	3212.2	82.5
0.104	0.201	0.264	0.430	0.30	3193.8	89.1
0.111	0.177	0.235	0.476	0.00	3188.4	81.8
0.111	0.177	0.235	0.476	0.30	3177.1	89.3
0.101	0.237	0.184	0.477	0.00	3138.4	80.3
0.101	0.237	0.184	0.477	0.35	3142.4	89.7

Table s1. Maximum CRI obtainable from metameric mixes of quad blends based on #246, #2194, #2288, and #2345. Comparison with no halo addition. Quad blends listed in order of increasing #2194 content. LWX color point. Part 2

Quad-blend content as fractional SPD(#XXXX)				Halo fract.	Lumens	CRI
#246	#2194	#2288	#2345			
0.100	0.246	0.176	0.477	0.00	3130.6	80.1
0.100	0.246	0.176	0.477	0.35	3137.6	89.8
0.086	0.329	0.104	0.478	0.00	3060.9	77.8
0.086	0.329	0.104	0.478	0.40	3096.8	90.2
0.085	0.337	0.098	0.479	0.00	3054.5	77.6
0.085	0.337	0.098	0.479	0.40	3093.0	90.3
0.083	0.351	0.086	0.479	0.00	3042.5	77.1
0.083	0.351	0.086	0.479	0.40	3085.7	90.3
0.075	0.397	0.047	0.480	0.00	3004.7	75.7
0.075	0.397	0.047	0.480	0.40	3063.1	90.2
0.066	0.452	0.00	0.480	0.00	2958.3	73.8
0.066	0.452	0.00	0.480	0.45	3044.9	90.4

DOCID: <EP___0595527A1_I_>

Table s2. Effect of adding the LWX halo-blend to LWX quad-blends.

QUAD blend: 0.140 (#246); 0.000 (#2194); 0.386 (#2288); 0.473 (#2345)
LWX halo-blend: 0.120 (#4381); 0.796 (#4459); 0.084 (#4300).

Halo fraction	Quad fraction	Lumens	CRI
0.00	1.00	3336.2	85.44
0.10	0.90	3317.6	87.25
0.15	0.85	3308.3	87.62
0.20	0.80	3299.1	87.81
0.25	0.75	3289.8	87.72
0.30	0.70	3280.5	87.05
0.35	0.65	3271.2	85.78
0.40	0.60	3262.0	84.29
0.45	0.55	3252.7	82.60
0.50	0.50	3243.4	80.76
1.00	0.00	3150.6	58.83

Table s3. Effect of adding the LWX halo-blend to LWX quad-blends.

QUAD blend: 0.066 (#246); 0.452 (#2194); 0.000 (#2288); 0.481 (#2345)
LWX halo-blend: 0.120 (#4381); 0.796 (#4459); 0.084 (#4300).

Halo fraction	Quad fraction	Lumens	CRI
0.00	1.00	2958.4	73.82
0.10	0.90	2977.6	78.72
0.15	0.85	2987.2	80.96
0.20	0.80	2996.9	83.09
0.25	0.75	3006.5	85.12
0.30	0.70	3016.1	87.08
0.35	0.65	3025.7	88.68
0.40	0.60	3035.3	89.87
0.45	0.55	3044.9	90.43
0.50	0.50	3054.5	88.82
1.00	0.00	3150.6	58.83

3. Blends of #246; #2288; #2345, #290.

Cost considerations require that the content of the expensive #2345 phosphor be minimized in blends. This could be achieved by adding to the combination of phosphors #246, #2288, and #2345 an inexpensive red-emitting material, such as phosphor #290.

Accordingly, Table tr1 gives an overview of the predicted performance (lumens and CRI) of quad blends containing #246, #2288, #2345, and #290. As in the previous cases, the metameric mixes with the highest CRI are also indicated, where appropriate.

The highest CRI (87.7 at ~3,180 lumens) is obtained in the presence of #290 when $c_{\#290}$=0.115, and for a 15% mix with the halo blend (Table tr2 and Figure iii1). For $C_{\#290}$=0.115, halo admixing up to ~0.3 increases the blend CRI. The lumen output of the metameric mixes decreases linearly with the halo content.

Table tr1. Maximum CRI obtainable from metameric mixes of quad blends based on #246, #2288, #2345 and #290. Comparison with no halo addition. Quad blends listed in order of increasing #290 content. LWX color point. Part 1.

Quad-blend content as fractional SPD(#XXXX)				Halo fract.	Lumens	CRI
#246	#2288	#2345	#290			
0.140	0.386	0.473	0.000	0.00	3336.3	85.4
0.140	0.386	0.473	0.000	0.20	3299.2	87.8
0.131	0.354	0.398	0.115	0.00	3186.0	86.6
0.131	0.354	0.398	0.115	0.15	3180.7	87.7
0.122	0.320	0.315	0.242	0.00	3019.1	87.0
0.112	0.283	0.227	0.337	0.00	2841.9	87.0
0.102	0.247	0.142	0.507	0.00	2672.3	86.0
0.100	0.237	0.118	0.544	0.00	2623.7	85.3

Table tr1. Maximum CRI obtainable from metameric mixes of quad blends based on #246, #2288, #2345 and #290. Comparison with no halo addition. Quad blends listed in order of increasing #290 content. LWX color point. Part 2.

Quad-blend content as fractional SPD(#XXXX)				Halo fract.	Lumens	CRI
#246	#2288	#2345	#290			
0.095	0.219	0.076	0.609	0.00	2539.2	83.9
0.090	0.201	0.031	0.677	0.00	2450.4	82.2
0.088	0.196	0.018	0.697	0.00	2424.2	81.6
0.086	0.188	0.000	0.725	0.00	2386.9	80.7

Table tr2. Effect of adding the LWX halo-blend to LWX quad-blends.

QUAD blend: 0.131 (#246); 0.355 (#2288); 0.398 (#2345); 0.115 (#290)
LWX halo-blend: 0.120 (#4381); 0.796 (#4459); 0.084 (#4300).

Halo fraction	Quad fraction	Lumens	CRI
0.00	1.00	3186.0	86.57
0.10	0.90	3182.4	87.49
0.15	0.85	3180.7	87.67
0.20	0.80	3178.9	87.58
0.25	0.75	3177.1	86.93
0.30	0.70	3175.4	85.74
0.35	0.65	3173.6	84.35
0.40	0.60	3171.8	82.78
0.45	0.55	3170.1	81.07
0.50	0.50	3168.3	79.26
1.00	0.00	3150.6	58.83

4. Blends containing Gd pentaborate:Ce;Mn as the red emitter.

Compared with the emission from phosphor #290 (Figure s6) the emission from the pentaborate[de1,de2] phosphor (L93S) is shifted to longer wavelengths and peaks at ~630nm (Figure s10). Starting from a tri-blend containing #246, #2288, and the pentaborate, phosphor #2194 is gradually added. This produces a monotonic drop in lumens and CRI, with the latter ultimately slumping down to ~71.6 from the initial value of 82.5 (Table ls0 and Figure fl1).

The metameric mixing raises both lumen out and CRI, the latter way above the value of 90. Details on the effect of the metameric mixing are listed in the summary Table ls1, and in Figure fl2 for the end-of-series novel formulation:

$$0.015 \cdot SPD(\#246) + 0.343 \cdot SPD(\#2194) + 0.641 \cdot SPD(L93S) \quad (6)$$

Table Is0. Quad blends based on #246, #2194, #2288 and L93S, in order of increasing #2194 content. LWX color point.

Quad-blend content as SPD(#XXXX)				Lumens	CRI
#246	#2194	#2288	L93S		
0.071	0.000	0.294	0.633	2653.4	82.5
0.063	0.054	0.248	0.634	2606.9	82.0
0.057	0.088	0.218	0.635	2577.2	81.5
0.054	0.104	0.205	0.635	2563.9	81.2
0.042	0.176	0.143	0.637	2501.8	79.2
0.041	0.181	0.138	0.637	2497.3	79.0
0.030	0.248	0.081	0.639	2439.9	76.2
0.029	0.257	0.074	0.639	2432.1	75.8
0.028	0.263	0.068	0.639	2427.0	75.5
0.022	0.300	0.037	0.640	2395.2	73.8
0.015	0.343	0.000	0.641	2358.1	71.6

Table Is1. Maximum CRI obtainable from metameric mixes of quad blends based on #246, #2194, #2288 and L93S. Comparison with no halo addition. Quad blends listed in order of increasing #2194 content. LWX color point. Part 1.

Quad-blend content as fractional SPD(#XXXX)				Halo fract.	Lumens	CRI
#246	#2194	#2288	L93S			
0.071	0.000	0.294	0.633	0.00	2653.4	82.5
0.071	0.000	0.294	0.633	0.20	2752.8	87.1
0.063	0.054	0.248	0.634	0.00	2606.9	82.0
0.063	0.054	0.248	0.634	0.20	2715.6	88.1
0.057	0.088	0.218	0.635	0.00	2577.2	81.5
0.057	0.088	0.218	0.635	0.20	2691.9	88.6
0.054	0.104	0.205	0.635	0.00	2563.9	81.2
0.054	0.104	0.205	0.635	0.25	2739.9	88.9
0.042	0.176	0.143	0.637	0.00	2501.8	79.2
0.042	0.176	0.143	0.637	0.25	2664.0	90.0
0.041	0.181	0.138	0.637	0.00	2497.3	79.0
0.041	0.181	0.138	0.637	0.25	2660.6	90.1

Table Is1. Maximum CRI obtainable from metameric mixes of quad blends based on #246, #2194, #2288 and L93S. Comparison with no halo addition. Quad blends listed in order of increasing #2194 content. LWX color point. Part 2.

Quad-blend content as fractional SPD(#XXXX)				Halo fract.	Lumens	CRI
#246	#2194	#2288	L93S			
0.030	0.248	0.081	0.639	0.00	2439.9	76.2
0.030	0.248	0.081	0.639	0.30	2653.2	91.0
0.029	0.257	0.074	0.639	0.00	2432.1	75.8
0.029	0.257	0.074	0.639	0.30	2647.1	91.1
0.028	0.263	0.068	0.639	0.00	2427.0	75.5
0.028	0.263	0.068	0.639	0.30	2644.1	91.2
0.022	0.300	0.037	0.640	0.00	2395.2	73.8
0.022	0.300	0.037	0.640	0.30	2621.9	91.5
0.015	0.343	0.000	0.641	0.00	2358.1	71.6
0.015	0.343	0.000	0.641	0.35	2635.5	91.9

Table ls2. Effect of adding the LWX halo-blend to LWX quad-blends.

QUAD blend: 0.015 (#246); 0.343 (#2194); 0.000 (#2288); 0.641 (L93S)
LWX halo-blend: 0.120 (#4381); 0.796 (#4459); 0.084 (#4300).

Halo fraction	Quad fraction	Lumens	CRI
0.00	1.00	2358.1	71.60
0.05	0.95	2397.7	75.84
0.10	0.90	2437.3	79.90
0.15	0.85	2477.0	83.76
0.20	0.80	2516.6	87.04
0.25	0.75	2556.2	89.75
0.30	0.70	2595.9	91.60
0.35	0.65	2635.5	91.85
0.40	0.60	2675.1	90.54
0.45	0.55	2714.7	88.55
0.50	0.50	2754.4	86.13
1.00	0.00	3150.6	58.83

5. Blends of #246; #2194; #2345, and #290.

The quad blends considered next contain the two red emitters (#2345 and #290), as in the previous blends, the usual #246 as blue emitter, and #2194 as the green emitter. The results for the quad blends and their metameric mixes are summarized in Table tw1. In the absence of #290 the tri-blend brightness is of ~2,958 lumens with a CRI of 73.8 (first row of Table tw1). The addition of #290 improves dramatically the CRI, up to 90, but exacts a toll in brightness, mainly because the replacement of #2345 by the relatively low-brightness #290 phosphor.

Some of the lumen losses can be recouped by halo addition. In all cases CRI values of 90 and more can be reached. For the particular case of the tri-blend with no #290, a substantial halo addition (45%) produces a CRI of 90.4 at 3045 lumens (row 2 of Table tr1). The pertinent SPD of such a metameric mix is shown in Figure dr1. This is the same tri-blend discussed in connection with the blends of #246, #2194, #2288, and #2345.

Table tw1. Maximum CRI obtainable from metameric mixes of quad blends based on #246, #2194, #2345 and #290. Comparison with no halo addition. Quad blends listed in order of increasing #2194 content. LWX color point. Part 1.

Quad-blend content as fractional SPD(#XXXX)				Halo fract.	Lumens	CRI
#246	#2194	#2345	#290			
0.066	0.452	0.481	0.000	0.00	2958.4	73.8
0.066	0.452	0.481	0.000	0.45	3044.9	90.4
0.064	0.420	0.415	0.100	0.00	2854.2	76.2
0.064	0.420	0.415	0.100	0.40	2972.8	90.6
0.061	0.382	0.338	0.217	0.00	2732.1	79.2
0.061	0.382	0.338	0.217	0.35	2878.6	90.7
0.059	0.344	0.259	0.337	0.00	2607.2	82.4
0.059	0.344	0.259	0.337	0.30	2770.3	90.8
0.058	0.338	0.246	0.356	0.00	2587.2	83.0
0.058	0.338	0.246	0.356	0.25	2728.1	90.6
0.055	0.284	0.136	0.524	0.00	2412.4	87.6
0.055	0.284	0.136	0.524	0.15	2523.1	90.8

Table tw1. Maximum CRI obtainable from metameric mixes of quad blends based on #246, #2194, #2345 and #290. Comparison with no halo addition. Quad blends listed in order of increasing #2194 content. LWX color point. Part 2.

Quad-blend content as fractional SPD(#XXXX)				Halo fract.	Lumens	CRI
#246	#2194	#2345	#290			
0.052	0.252	0.070	0.624	0.00	2307.9	89.7
0.052	0.252	0.070	0.624	0.10	2392.2	90.4
0.052	0.246	0.057	0.643	0.00	2288.4	89.9
0.052	0.246	0.057	0.643	0.05	2331.5	90.4
0.051	0.232	0.028	0.687	0.00	2242.9	90.1
0.050	0.218	0.000	0.731	0.00	2197.2	89.7

Some guidelines will be now outlined for the implementation of the present results into actual lamps. The basic results of the present application are:

1. The spectral profiles of SPD's that are characterized by a pre-assigned color point, and have associated specific values of lumens and CRI.
2. The way to construct such SPD's starting from the SPD of existing single-component lamps, by means of the mixing coefficients c_i introduced in eqs 3 and 4. Up to this point the derivation is rigorous.

1. From SPD fraction to phosphor-weight formulations.

From the viewpoint of the lamp technologist the type of photometric information embedded in the c_i mixing coefficients has to be translated into fractional weight composition for the individual phosphors in the blend.

Let us start with the simple assumption that the blend components represent completely randomized and non-interacting subsystems in the lamp, so that the blend output in lamps is the superposition of the contributions from the individual blend components. In such a case, if the single-lamp powder weights are the same, then the photometric c_i coefficients become identical to the fractional weight w_i of the individual phosphor-blend components.

With reference to Table b2, the phosphor weight in the single-component lamps is in practice not the same. Then the transition from SPD fractions to weight fractions is a simple matter of multiplying the SPD fractions c_i by the powder-weight of the corresponding lamp, and of re-normalizing, as shown below.

Let c_n be the photometric (SPD) fraction for blend component n, and s_n the phosphor powder-weight of the single-component lamp for blend component n (see Table b2). Then the blend fractions w_n in weight units are given by:

$$w_n = (c_n \cdot s_n) : (\Sigma_n c_n \cdot s_n) \quad (7)$$

with n=1,2,3, and 4.

An example of this simple transformation will be carri d for the entries of Table p1. The ensuing Table i1 is a modified version of Table p1, in the sense that each pair of rows gives the phosphor-blend compositions

expressed in c_i units (fraction of single-lamp SPD) in the top row, and in fractional-weight units in the bottom row.

Table 11. Quad blends for the LWX color-point (x=0.387 and y=0.391), based on phosphors #246, #2194, #2293, and #2345. Composition, blend weight (in grams) and predicted output in order of increasing #2194. Top row in row pairs: c_i mixing coefficients for the SPD's; bottom row: weight percent fraction in blends. Part 1.

#246	#2194	#2293	#2345	Blend weight	Lumens	CRI
0.134	0.000	0.476	0.389		3460.3	83.13
0.112	0.000	0.506	0.382	6.21	3460.3	83.13
0.125	0.061	0.411	0.401		3392.0	85.74
0.105	0.058	0.440	0.396	6.16	3392.0	85.74
0.117	0.115	0.355	0.412		3333.1	87.09
0.099	0.110	0.381	0.409	6.14	3333.1	87.09
0.104	0.201	0.264	0.430		3237.1	86.89
0.088	0.195	0.286	0.431	6.09	3237.1	86.89
0.101	0.220	0.244	0.433		3216.2	86.11
0.086	0.214	0.265	0.435	6.07	3216.2	86.11

Table i1. Part 2.

#246	#2194	#2293	#2345	Blend weight	Lumens	CRI
0.097	0.250	0.213	0.434		3182.7	84.76
0.084	0.244	0.233	0.439	6.03	3182.7	84.76
0.087	0.313	0.146	0.452		3112.0	81.76
0.075	0.307	0.160	0.458	6.02	3112.0	81.76
0.085	0.324	0.135	0.455		3100.8	81.22
0.073	0.317	0.148	0.461	6.02	3100.8	81.22
0.084	0.333	0.125	0.456		3091.0	80.77
0.073	0.327	0.137	0.463	6.01	3091.0	80.77
0.075	0.390	0.065	0.468		3027.0	77.67
0.065	0.385	0.072	0.478	5.97	3027.0	77.67
0.074	0.398	0.056	0.470		3017.9	77.21
0.064	0.393	0.062	0.480	5.97	3017.9	77.21
0.066	0.452	0.000	0.481		2958.3	73.82
0.058	0.448	0.000	0.493	5.94	2958.3	73.82

2. The linearized blend model of completely randomized, non-interacting blend components may turn out not to be realized in practice for a variety of reasons. Then the weight fractions listed in the previous Table may not exactly result in a lamp with the targeted color-point.

In such a case the target SPD (see for instance Figures i1 and dr1) can always be constructed on the basis of the information provided in the present application, namely from the component SPD's of Figures s1 to s10 and the c_i coefficients (and halo-mixing fractions in the case of m tameric mixes) listed in the preceding Tables.

Once the target SPD is thus constructed. it can be used as a bench-mark for the SPD obtained from the experimental lamps, in the sense that the blend composition of the test lamps can be slightly altered by trial-and-error, until the SPD's of the experimental lamps containing the modified blend converge to the bench-

mark SPD, and hence to the target color-point.

3. An alternative, more systematic approach, requiring the fabrication and photometric characterization of a single test lamp, is the following. Let $S_{targ}(\lambda_1)$ be the predicted SPD-intensity for the target blend-lamp at the wavelength λ_1, and $S_e(\lambda_1)$ the actual SPD-intensity observed in the test lamp containing a blend of weight-percent composition characterized by the w_i coefficients of eq.7. Let us assume that $S_e(\lambda_1) \neq S_{targ}(\lambda_1)$. Then one possible route to bring about the convergence of S_e to S_{targ} is the following.

At a given wavelength λ_m the output $S_e(\lambda_m)$ from the experimental lamp can be viewed as arising from the contribution of the component SPD's, here labelled $S_c(\lambda)$, each blend component contributing according to a factor $f_c(\lambda_m)$. So at the wavelength λ_m, one has for the test lamp:

$$\Sigma_c \, f_c(\lambda_m) \cdot S_c(\lambda_m) = S_e(\lambda_m) \quad (8)$$

with c=1, 2, 3, and 4.

We assume now that $f_c(\lambda_m) = f_c$, namely that the f_c factors are independent of wavelength, which is normally the case, unless, for instance, one of the phosphors absorbs the visible radiation emitted by another blend component

This means that if we choose four different wavelengths λ_m in the S_e output, we can set up three more relations such as eq. 8, that constitute together with eq. 8 a system of four linear equations in the four unknown f_c (with c=1,2,3 and 4). Such a system of linear equations is easily solved by means of a well-known procedure, Cramer's rule. The f_c quantities can be viewed as "effective mixing coefficients", compared to the c_i factors of eq. 3, 4 that are derived for the linear model of randomized, non-interacting blend components.

After deriving the f_c values, we use them to arrive at a modified blend formulation. In the corrected blend the following relation will apply at λ_m:

$$\Sigma_c \, g_c S_c(\lambda m) = S_{targ}(\lambda_m) \quad (9)$$

with c_i=1, 2, 3, and 4, and where $S_{targ}(\lambda_m)$ is now the target SPD, rather than the SPD of the test lamp, as in eq. 8. By a repeat of the previous procedure, after selecting three additional wavelengths in the SPD, we can derive again by Cramer's rule the unknown g_c factors, since the $S_c(\lambda_m)$ spectral profiles are known experimentally (see Figures s1 to s10), and the S_{targ}'s are derived in the present application.

Once the g_c factors have been obtained, we are still left with the problem of establishing a connection between these photometric g_c factors and a blend description in terms of the component fractional-weights. Such a relation, though, has been established for the f_c coefficients, since in the test lamp the f_c coefficients are associated with the fractional weights w_c of the blend components. In particular the f_c coefficient for the case of unit weight (1 gram) of component c is given by:

$$u_c = \frac{f_c}{w_c L_e} \quad (10)$$

with: u_c a power/weight equivalent with dimensions of Watts/(nm·grams); L_e the blend weight in grams for the test lamp; and w_c the weight fraction for component c.

Using eq. 10, the required weight W_c of component c that will satisfy eq. 9 will be then given by the expression:

$$g_c = \frac{f_c}{w_c L_e} \cdot W_c = u_c \cdot W_c \quad (11)$$

and re-arranging eq. 11 :

$$W_c = \frac{g_c}{u_c} \quad (12)$$

for the required weight of component c in the blend.

Going back to the mixing coefficients c_i of eqs. 3 and 4, their associated power/weight equivalent was $1/s_i$, with s_i the powder weight of the single-phosphor lamp containing component s_i. The ratio:

$$(1/s_C): u_c = (u_c \cdot s_c)^{-1} \quad (13)$$

of the predicted and observed power/weight equivalents is therefore a measure of the deviation from the linearized model of randomly-distributed, non-interacting phosphor blends. The expression $(u_c \cdot s_c)^{-1}$, which will be either greater or less than unity, can be viewed as a "utilization factor" of phosphor c in the particular phosphor blend under consideration.

4. Lamp configurations with two phosphor-layers.

W m ntion d earli r th high material costs associated with phosphors containing rare- arth lements. As a cost-cutting m asure th fluor sc nt-lamp industry fr qu ntly r s rts to depositing the phosphors in lamps as two successiv lay rs[ho1]. The first lay r, adjacent to th inner surfac of the glass bulb is generally a phosphor, or phosphor bl nd, consisting of inexpensive hal phosphate phosphors. Aft r drying this first

phosphor-layer must be insoluble in the suspension used to deposit the subsequent phosphor layer. The second phosphor layer is generally a tri-component blend of rare-earth-containing phosphors, of type #246, #2293 and #2345 in the specific instance of Sylvania lamps.

This top layer of premium phosphors efficiently intercepts and absorbs the UV radiation produced by the plasma, and so it can be applied in relatively thin layers. For example, when the top layer represent 20% in weight of the total phosphor content of the lamp, the resulting thin top layer ("skin coat") absorbs approximately 60% of the available UV radiation, the remaining being converted in the underlying halophosphate phosphor-layer.

As the thickness of the top layer increases, the fraction of total UV-radiation absorbed in the top layer increases, but so does the phosphor cost. At this stage the economy in phosphor cost has to be balanced against the higher manufacturing costs intrinsic to the two-phosphor-layer fabrication.

The results presented here on metameric mixes are applicable also to two-phosphor-layer lamp configurations in the following sense. In the two-phosphor-layer configuration the lamp output is the superposition of the output from the individual phosphor layers. The thickness of the top, or premium, phosphor-layer determines the fraction of available UV radiation to be converted in each individual layer.

The two-phosphor-layer configuration can therefore be viewed as an extreme case of the break-down, deliberately induced, of the model of randomized blend components.

We have already mentioned that in the "skincoat" configuration 60% of the available UV radiation is converted in the top layer, and 40% in the halophosphate layer. From the viewpoint of lamp output this is exactly equivalent to having a metameric mix of 60% tri- (or quad-) blend and 40% halo blend.

As a concrete example, we refer to Table p6, part 2. There are two metameric mixes based on 60% quad-blend containing #246, #2194. #2293. #235, and 40% halo-blend, such mixes providing CRI values of 90.4 and 90.5 respectively, at brightness levels exceeding 3,000 lumens. This type of output can either be achieved in a single-phosphor-layer configuration, or in a double-phosphor-layer configuration. In the latter case the required weight of the quad blend can be reduced to approximately a third, thus realizing a saving in phosphor costs. In the former case the manufacturing process is faster and less expensive.

Single-phosphor-layer lamps based on the results of the present application were fabricated at GTE US Lighting by C. Ford, L. Plante, and F. Taubner (Memo of Dec. 21st, 1988). One particular formulation was selected for testing, namely the mix listed as the last row of Table s1. Instead of phosphor #2194, a related phosphor type. #2196, with a slightly different output was used.

The fractional weight percent of the phosphor components for the tri-blend are listed in Table te1.

Table te1. Fractional-weight composition for the tri-blend utilized in the lamp tests.

	#246	#2194	#2345
Calculated (Table I1)	0.058	0.448	0.493
Used in the lamp tests	0.06	0.46	0.48

Three test lamps were built, containing respectively the tri-blend of Figure te1, the halophosphate, and the metameric mix. The SPD of the lamp containing the tri-blend is shown in Figure le1. The lamp CRI was 65.6. The SPD of the halophosphate test-lamp is given in Figure le2. Its CRI was 58.8. The SPD of Figure le2 should be compared with the predictions of Figure hb1.

The metameric mix employed in the test lamp consisted of 45% halophosphate and 55% quad-blend. as per the last row of Table s1. The test lamp SPD is displayed in Figure le3. From the SPD one can derive color coordinates of 0.383 and 0.374, and a CRI of 90.4. The output brightness was 3,086 lumens at 0 hrs and 3,011 lumens at 100 hours, with a 0-100 hrs maintenance of 97.6%. The predictions of Table s1 were for 3,045 lumens at 100hrs and a CRI of 90.4. The SPD of the test lamp of Figure le3 should be compared with the calculated SPD of Figure dr1. The agreement is excellent. Minor differences in fine-structure components are due to the different spectral resolution of the detectors used for the measurements of the SPD of Figures s1 to s10, and for the measurement of the SPD of Figure le3.

The location of the color points of the three experimental lamps is shown in Figure bl1 relatively to the planckian locus. The color point of th metameric mix, indicated in the Figure as MM, is seen to fall nicely on the Planckian (black-body) locus.

Claims

1. A fluorescent lamp having a plurality of lamp phosphors for converting ultraviolet radiation to visible illumination, characterised in that the lamp phosphor comprises a plurality of metameric blends.

2. A fluorescent lamp as claimed in claim 1 characterised in that each of said blends of lamp phosphors has substantially identical color coordinates.

3. A fluorescent lamp as claimed in claim 1 or 2 characterised in that each of said lamp phosphors has a different Spectral Power Distribution.

4. A fluorescent lamp as claimed in claim 1, 2 or 3 characterised in that one of said blends of lamp phosphors comprise a quad-phosphor blend.

5. A fluorescent lamp as claimed in claim 4 characterised in that said quad-phosphor blend comprising a red color emitting phosphor component having a visible emission spectrum principally in the 590 to 630 nm wavelength range, blue color emitting phosphor component having an emission spectrum principally in the 430 to 490 nm wavelength range, a green color emitting phosphor component having emission spectrum principally in the 500 to 570 nm wavelength range, and an additional phosphor having a visible emission spectrum.

6. A fluorescent lamp as claimed in claim 5 wherein said additional phosphor comprises a red or green emitting phosphor component.

7. A fluorescent lamp as claimed in any of claims 4 to 6 characterised in that another one of said blends of lamp phosphors comprises alkaline earth metal halophosphate phosphors.

8. A fluorescent lamp as claimed in claim 7 characterised in that a layer of said alkaline earth metal halophosphate phosphors is on the interior surface of the glass envelope and said quad blend is a separate layer directly adjacent said layer of alkaline earth metal halophosphate phosphor.

9. A fluorescent lamp as claimed in claim 7 or 8 characterised in that the amount of said quad-phosphor blend is from about 10 percent and 50 weight percent of the total combined phosphor weight of the phosphor layers.

10. A fluorescent lamp as claimed in any preceding claim characterised in that said visible light has predetermined x and y values of ICI coordinates wherein the x value is in the range of 0.35 to 0.45, and said y value is in the range of 0.375 to 0.425.

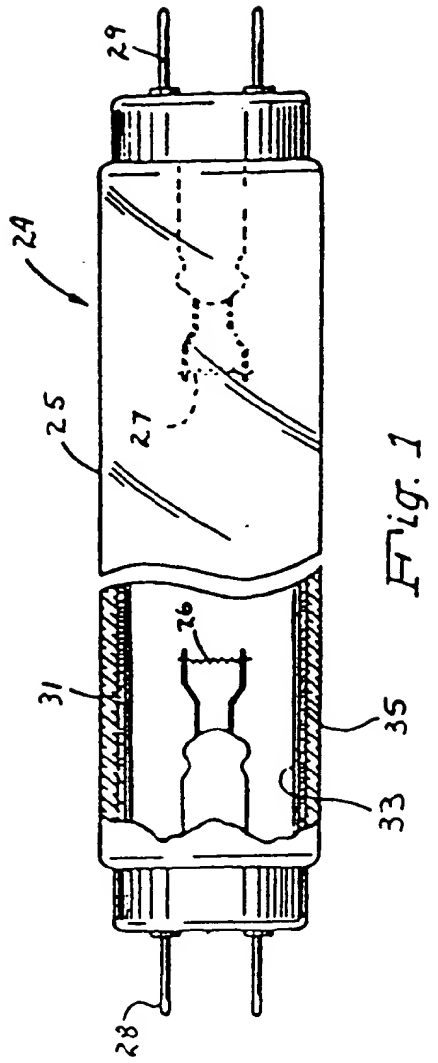

Fig. 1

Fig. S1

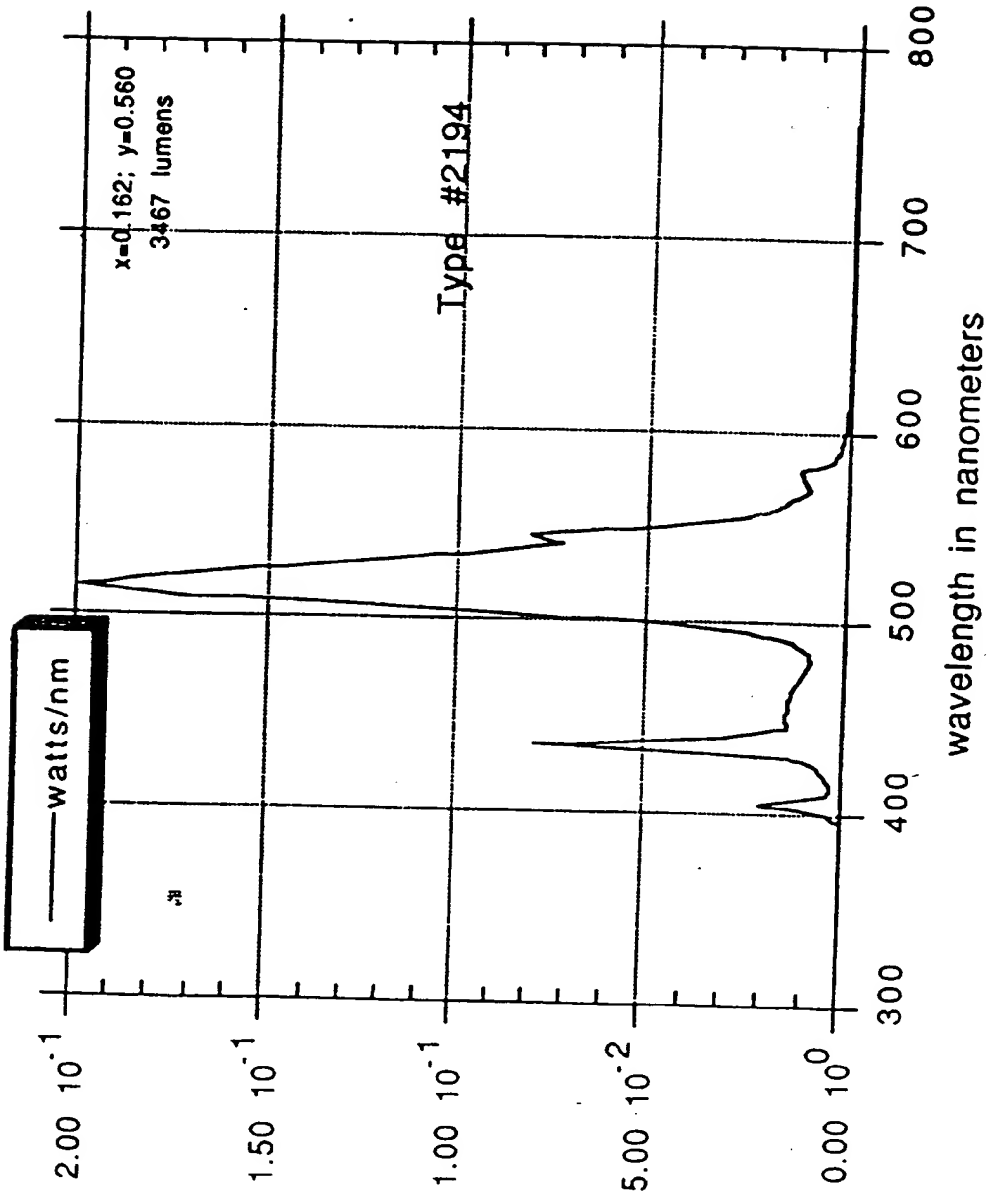

FIG. S2

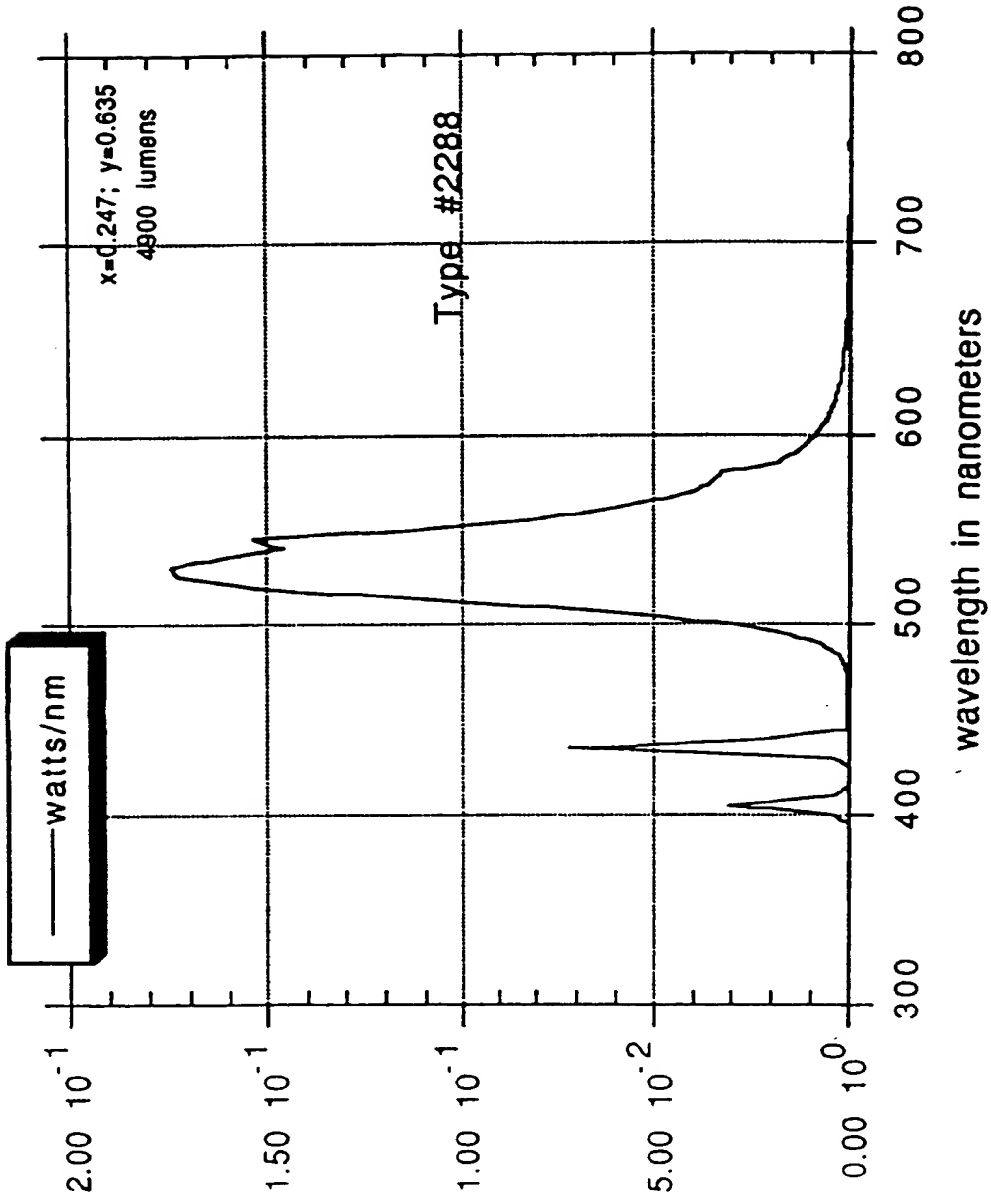

FIG. 53

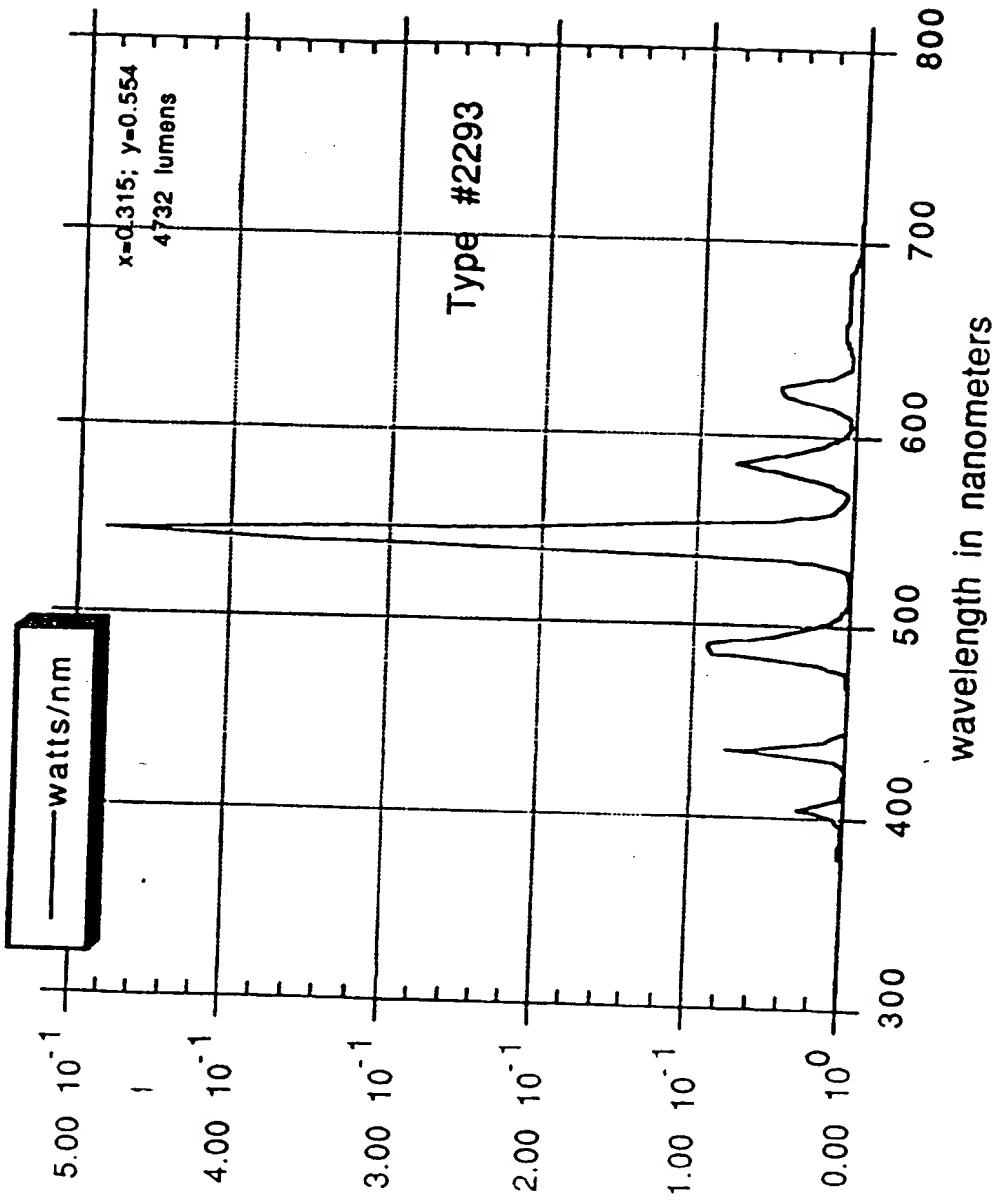

FIG. 54

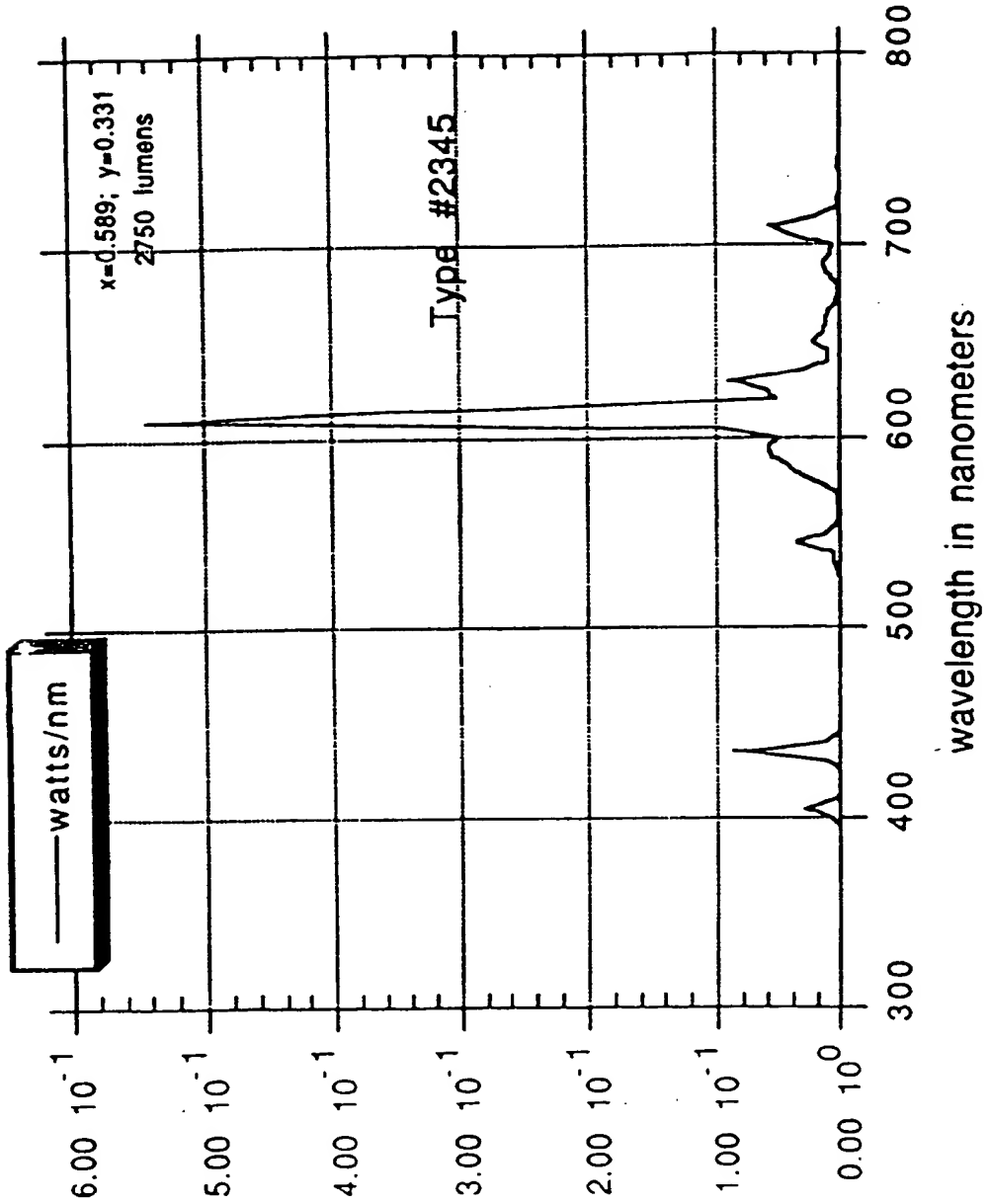

Fig. 55

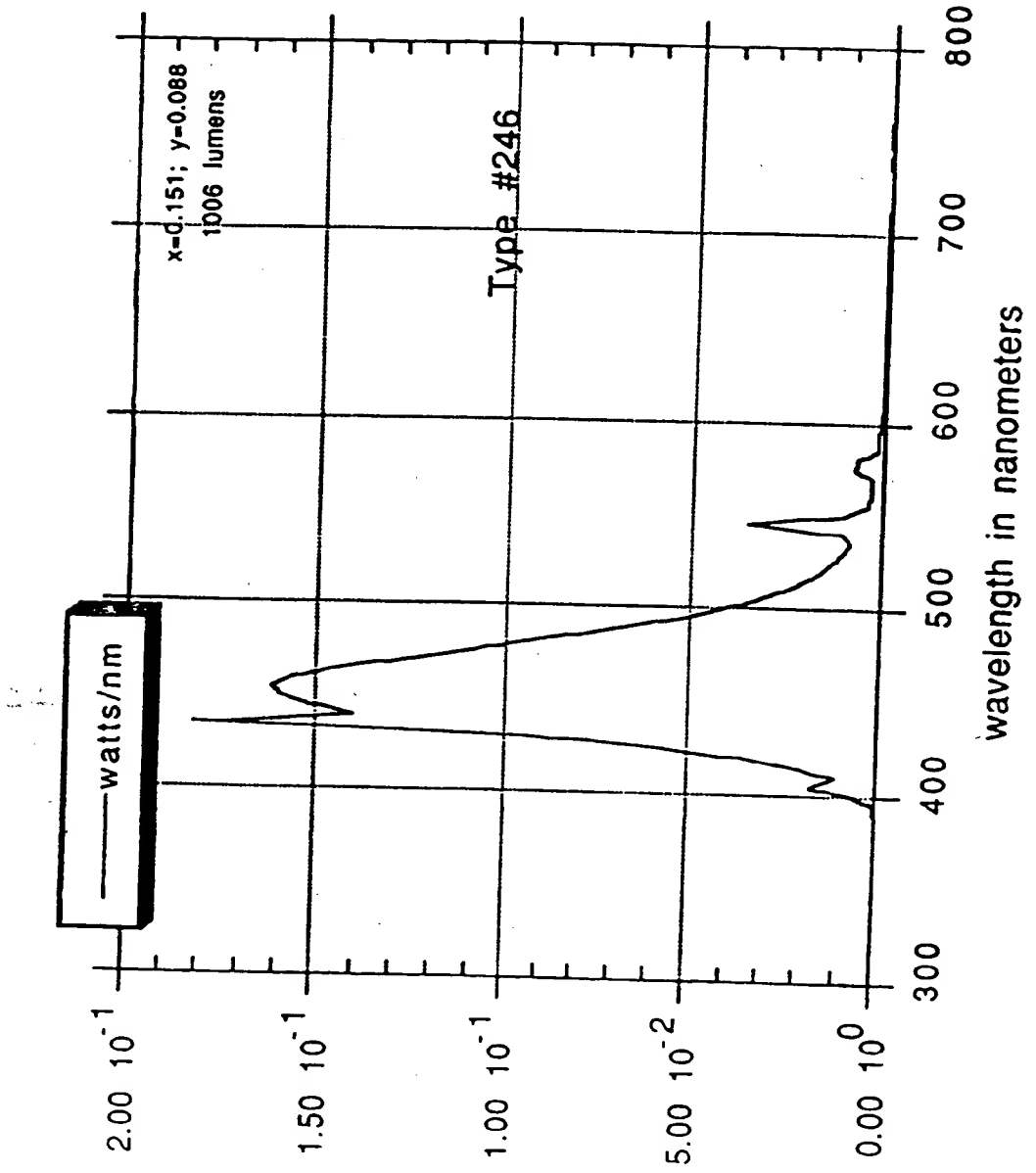

FIG. 56

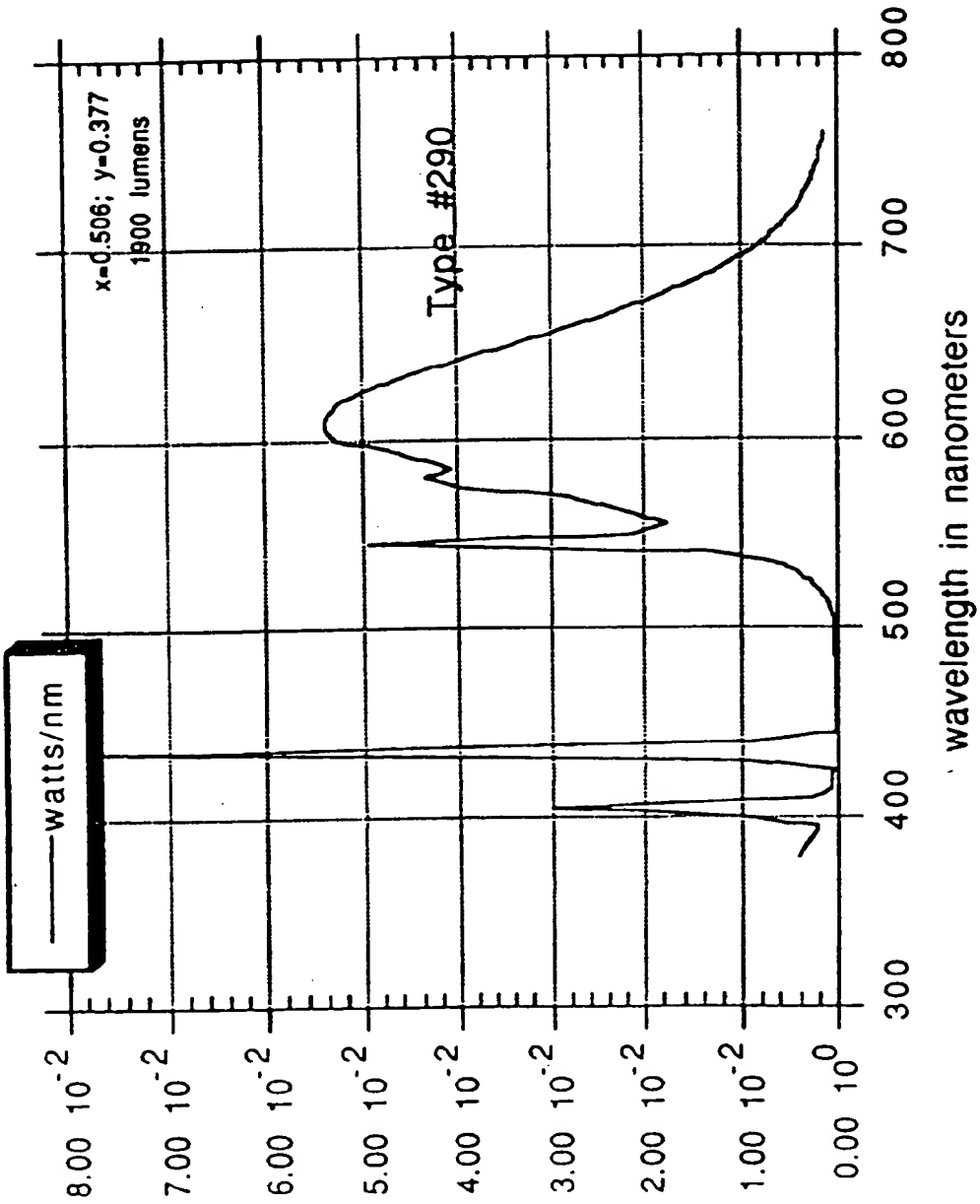

FIG. 57

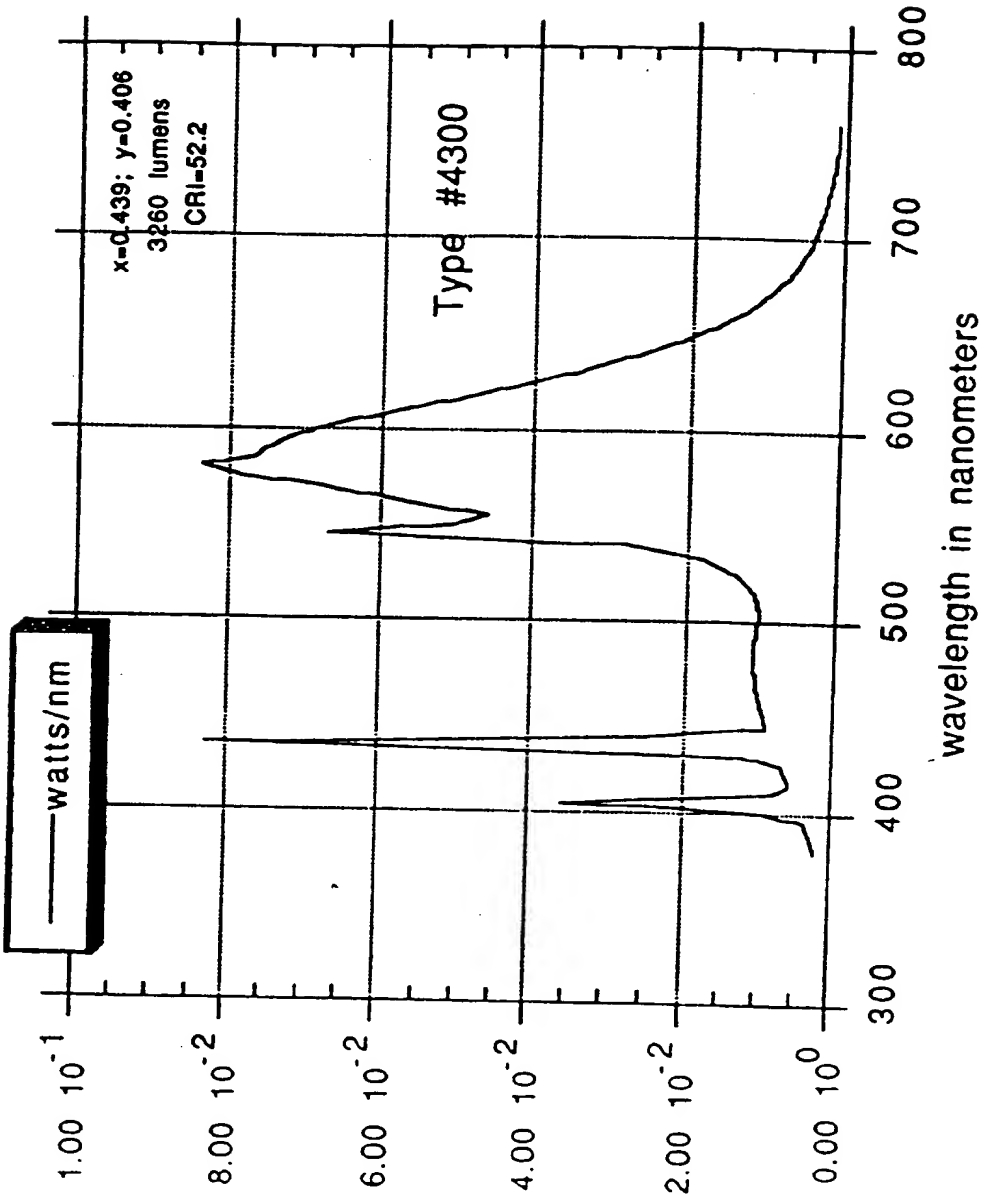

FIG. 58

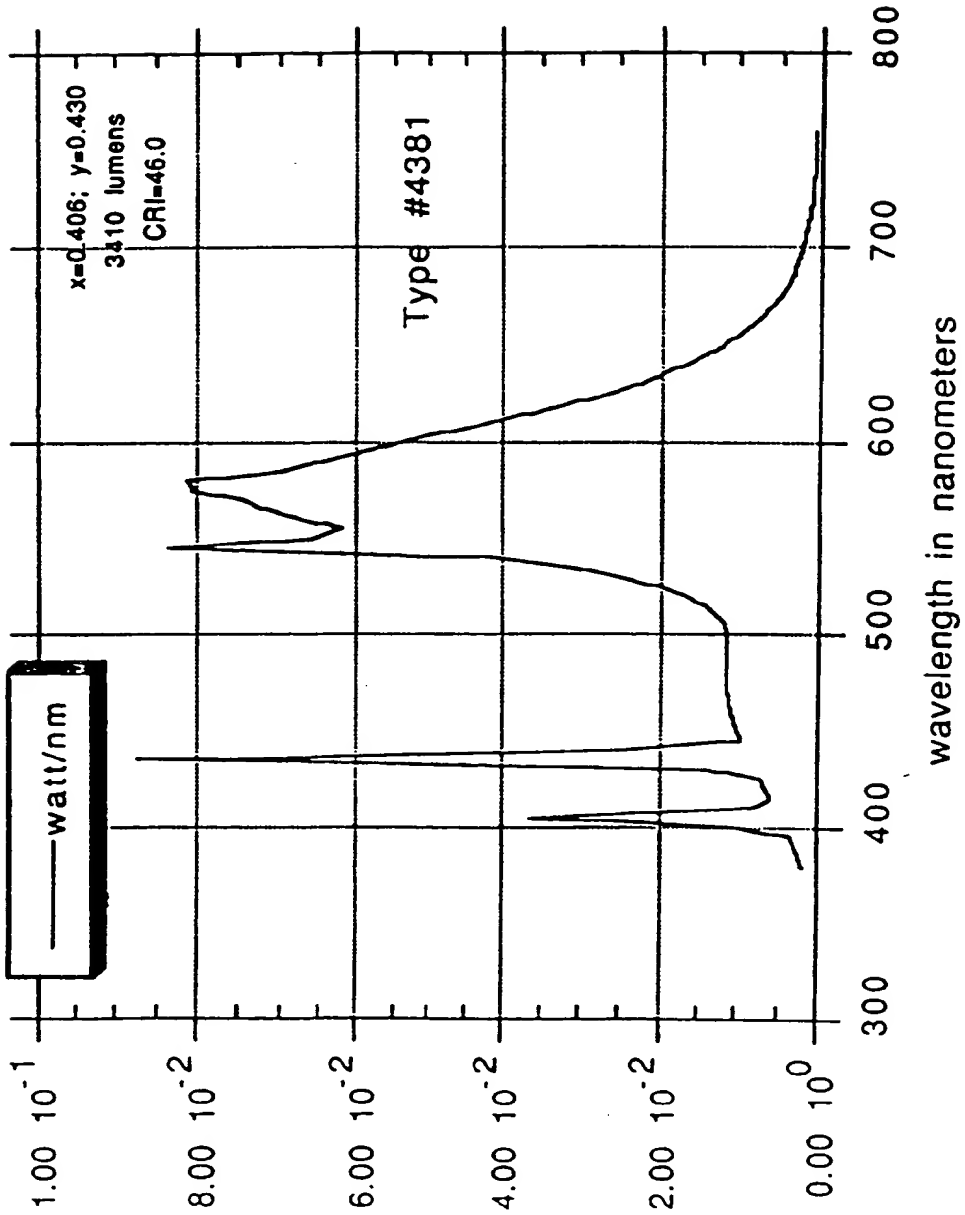

Fig. 89

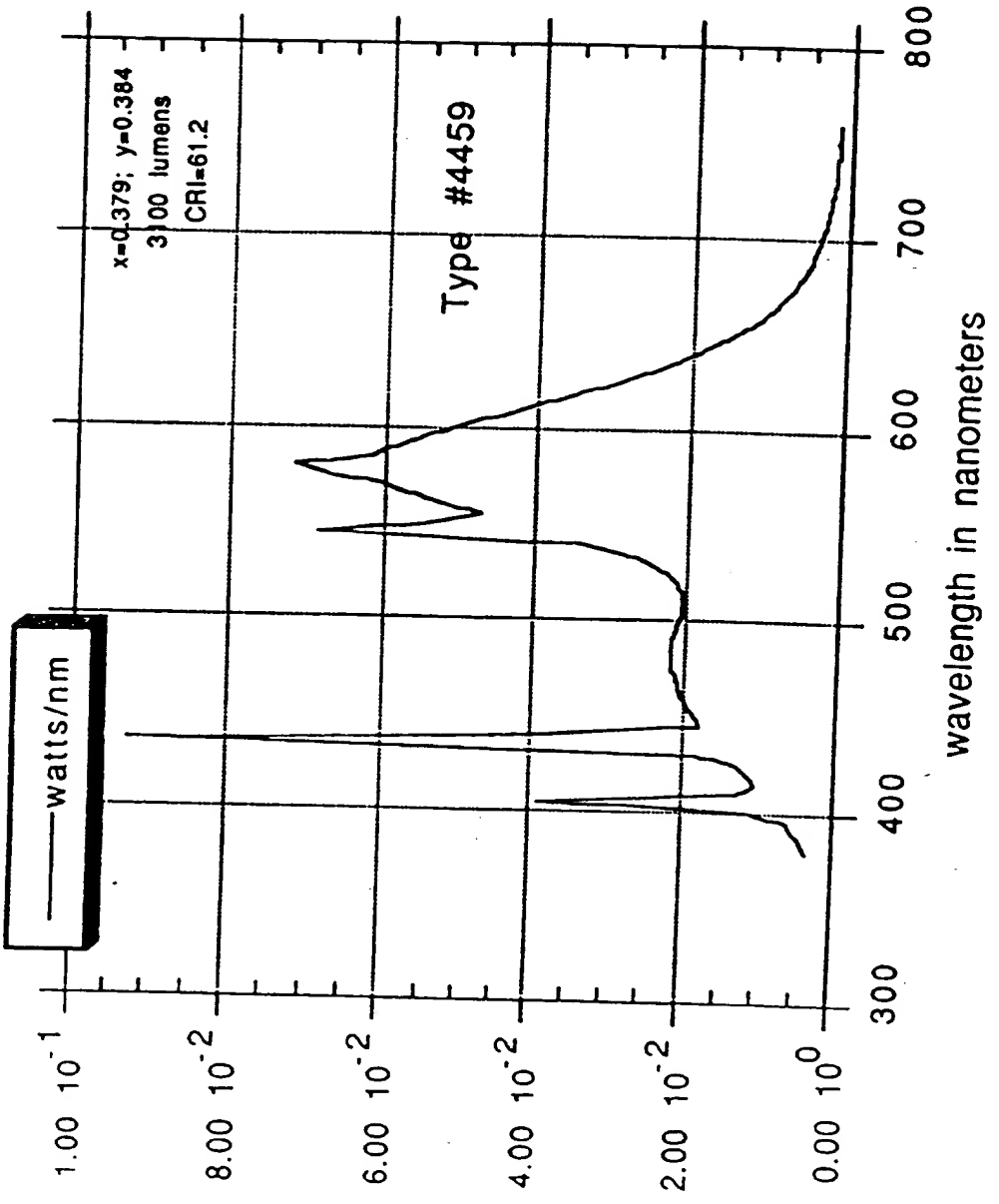

Fig. S10

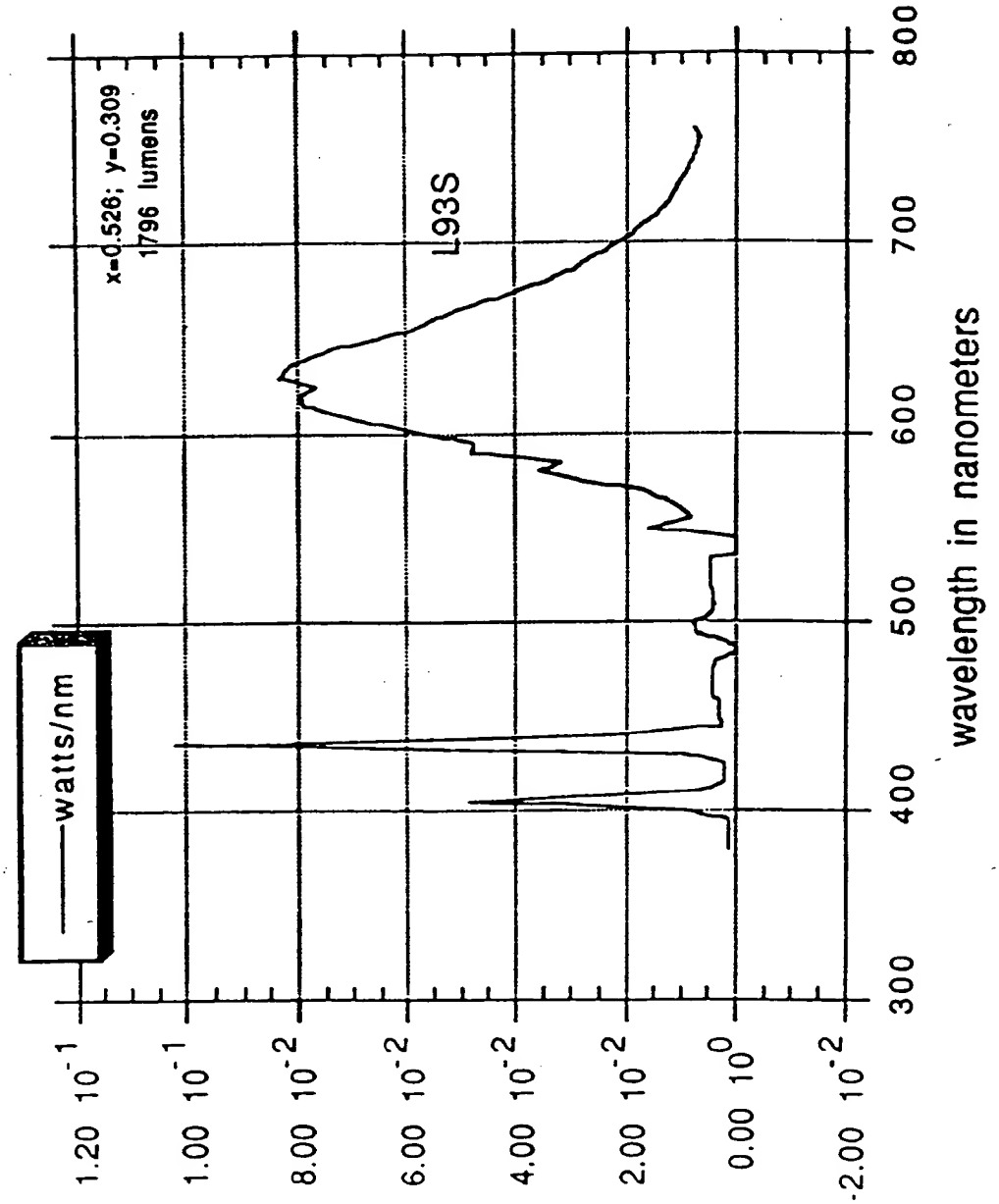

Fig. 46.1

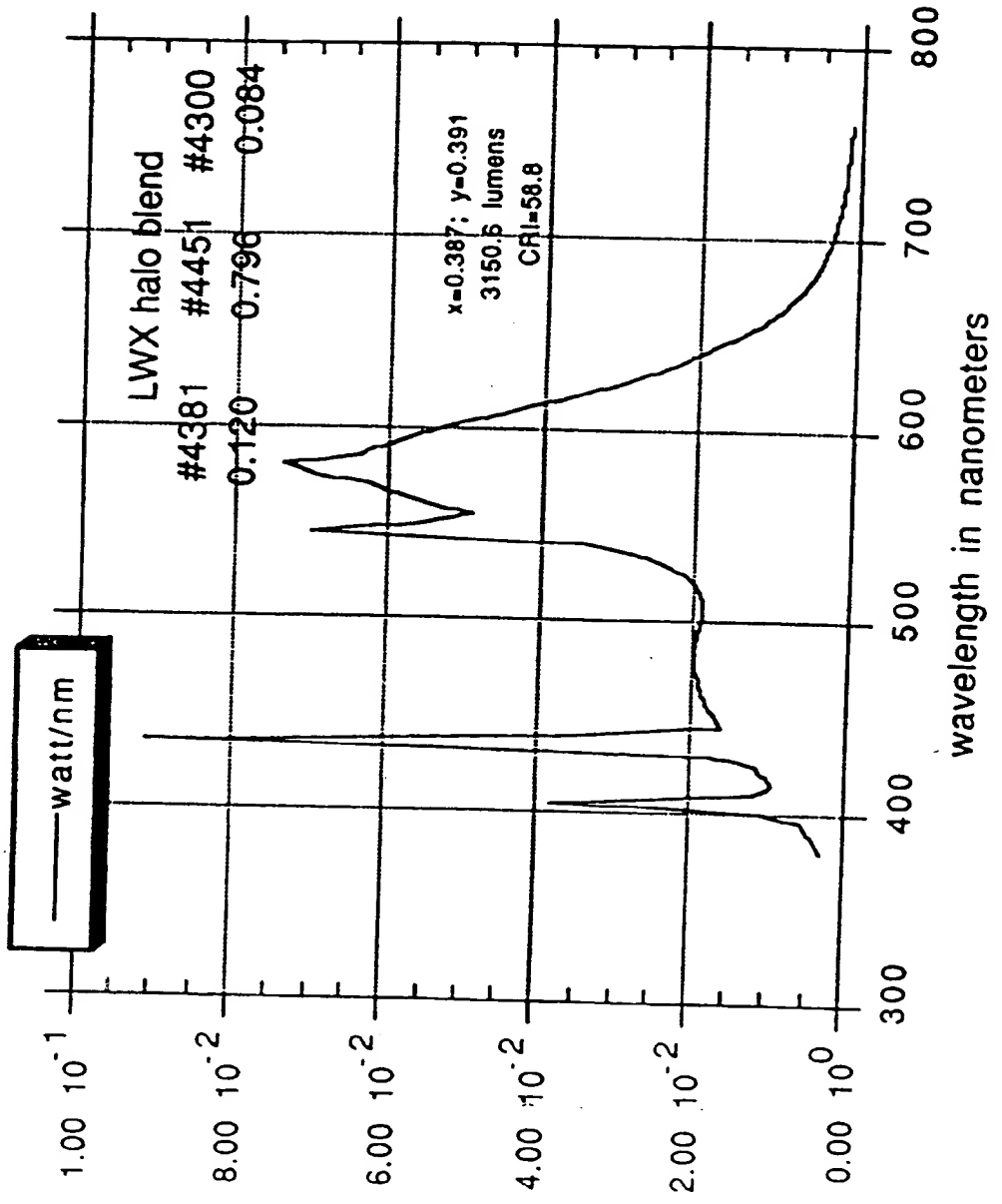

Fig. 10

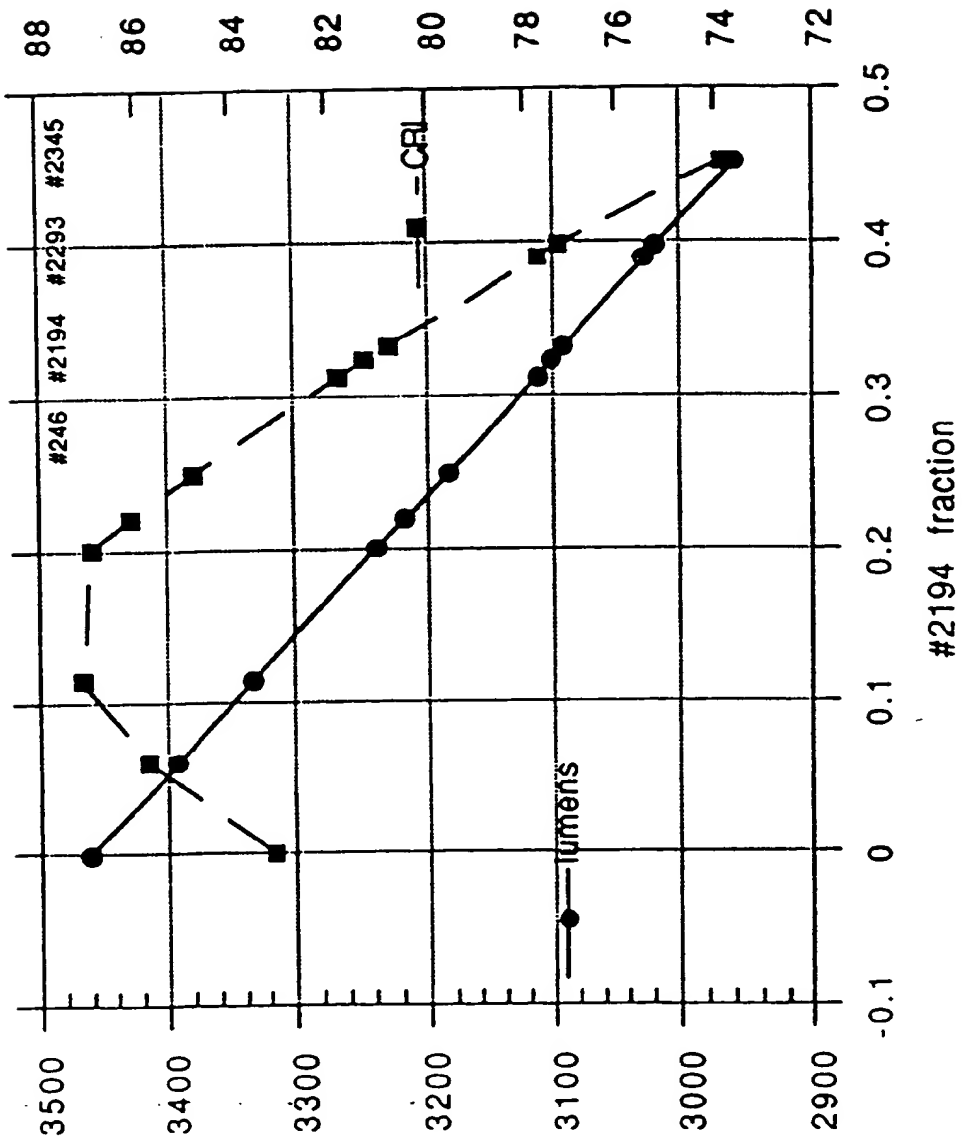

Fig. 11

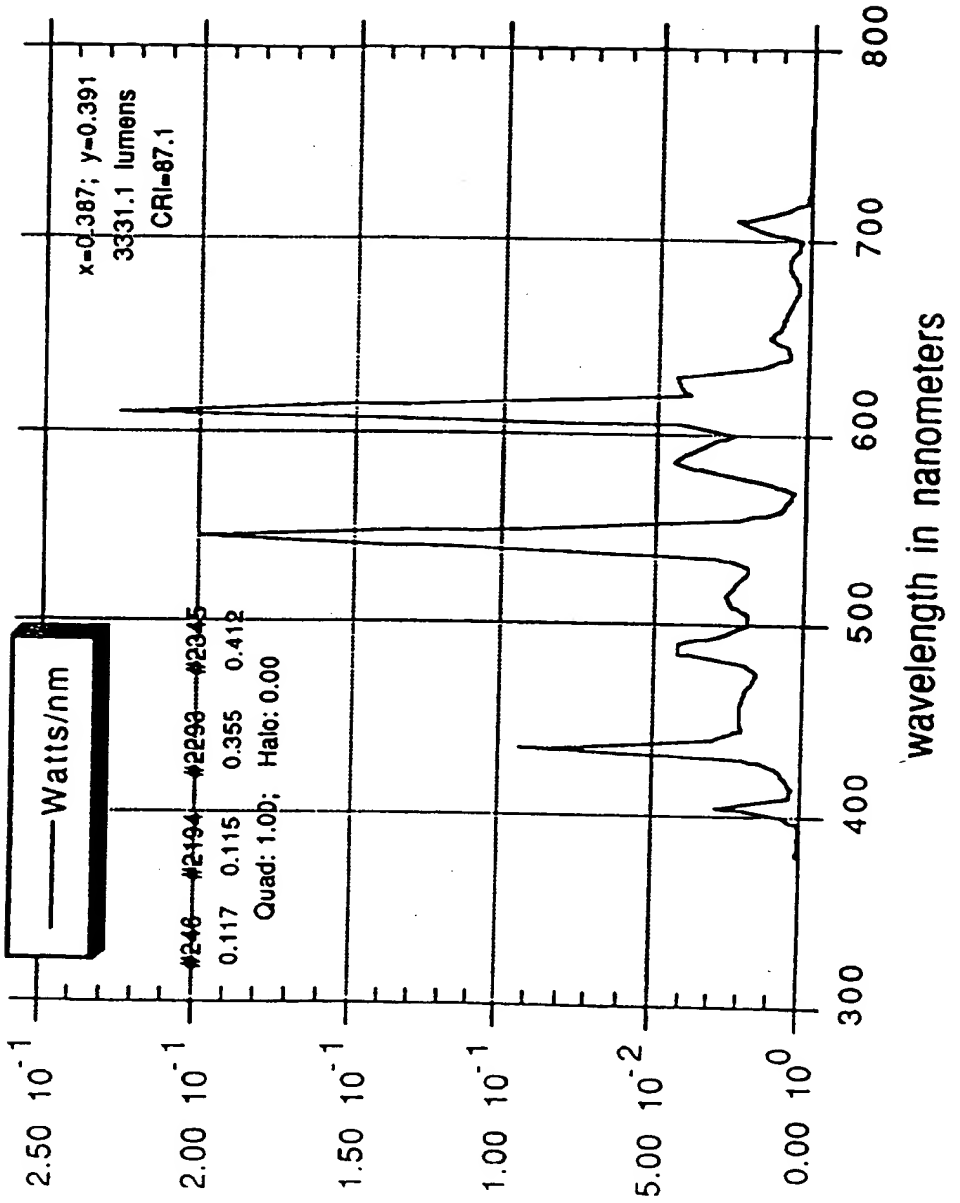

Fig. 12

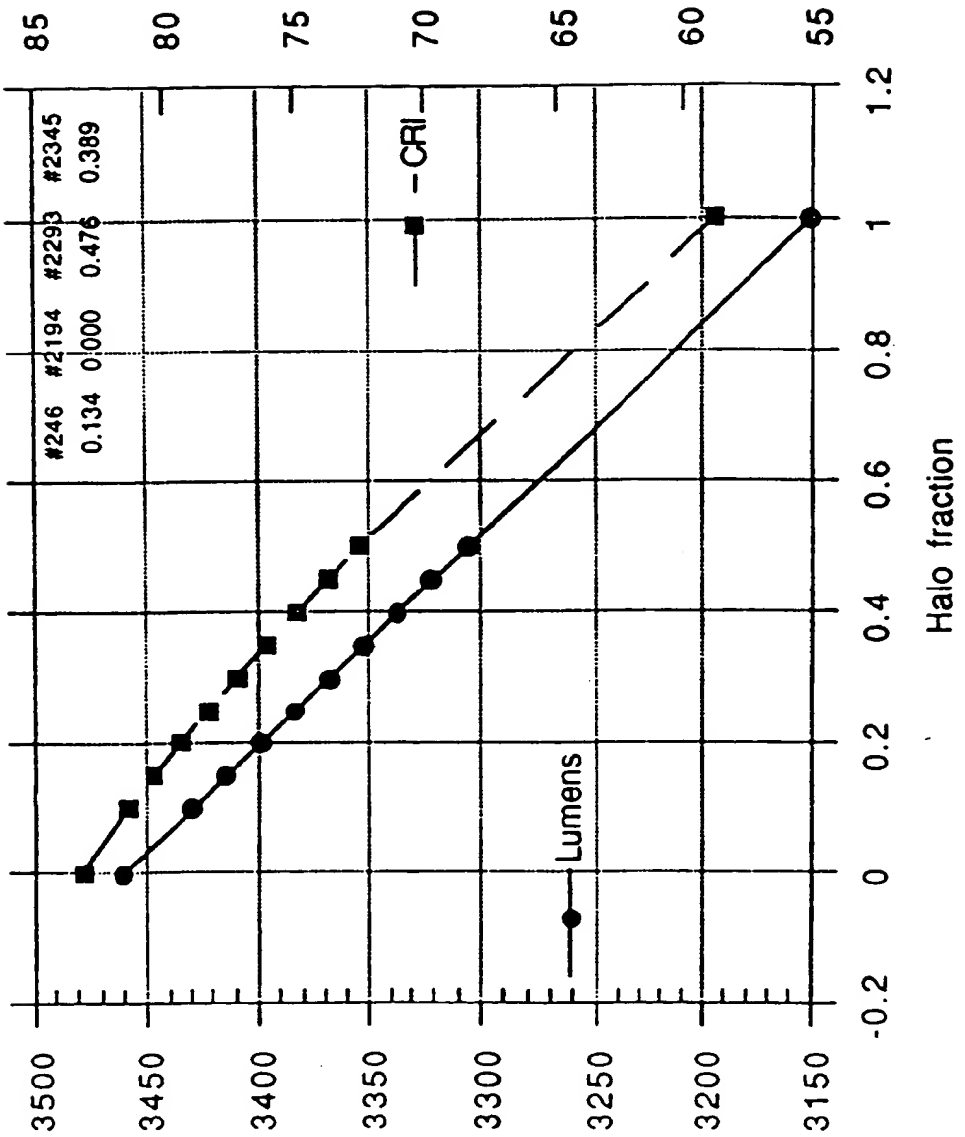

Fig. 13

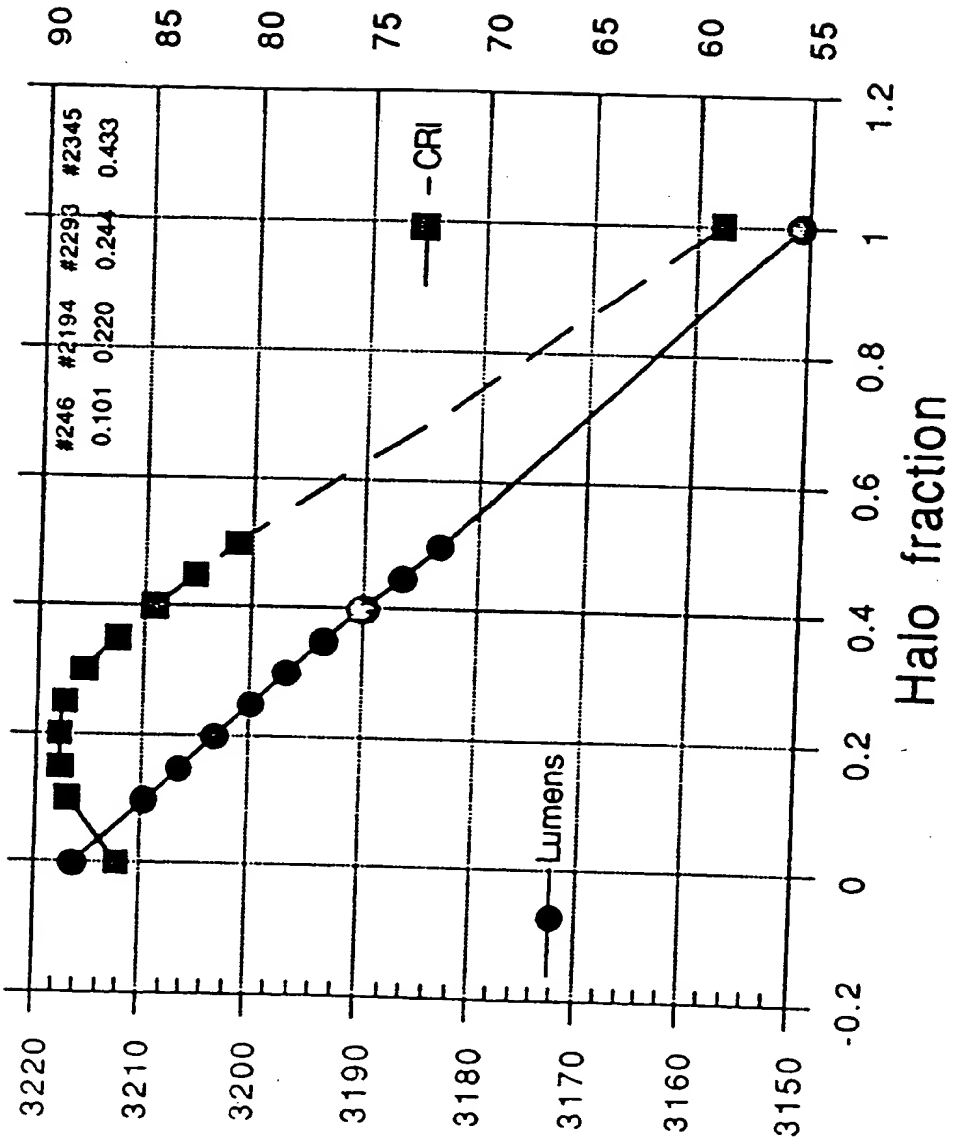

Fig. 14

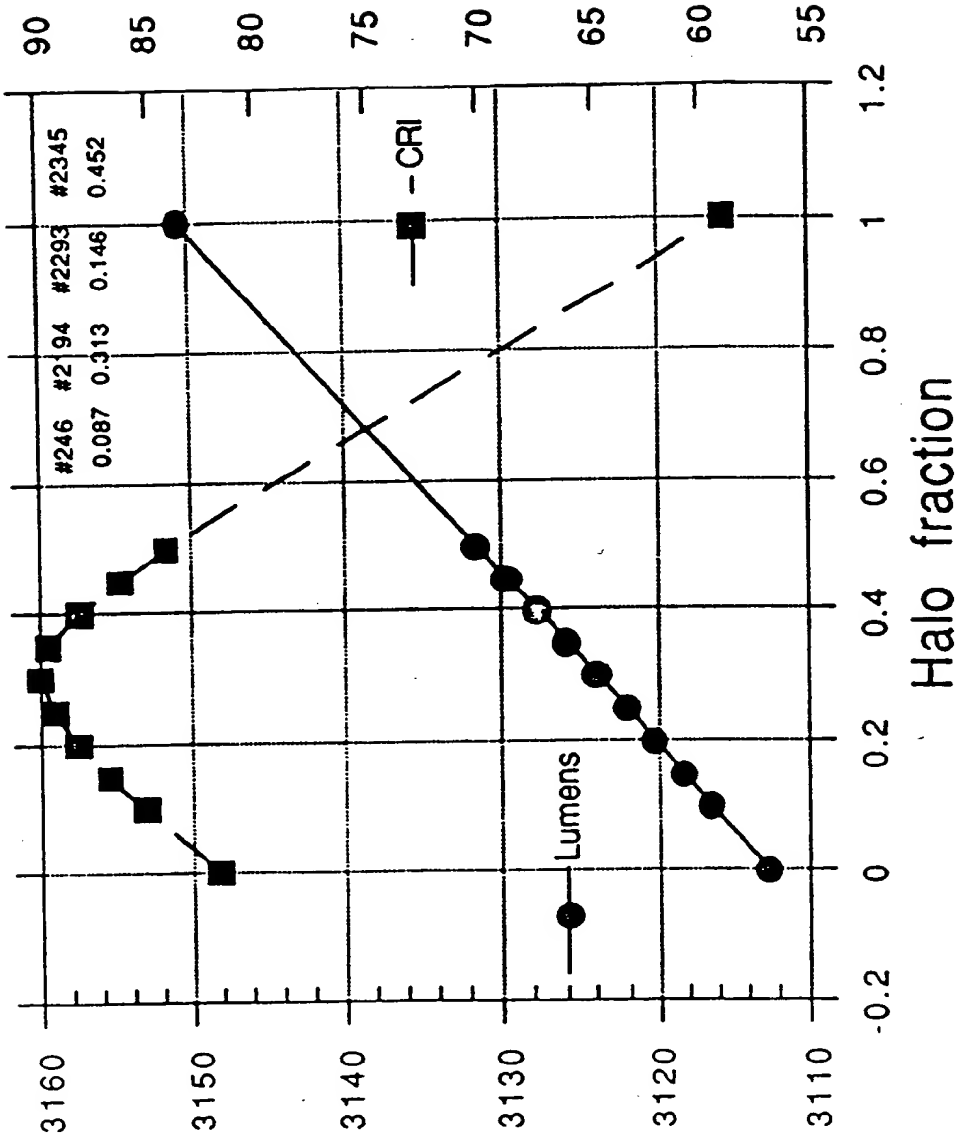

Fig. 11

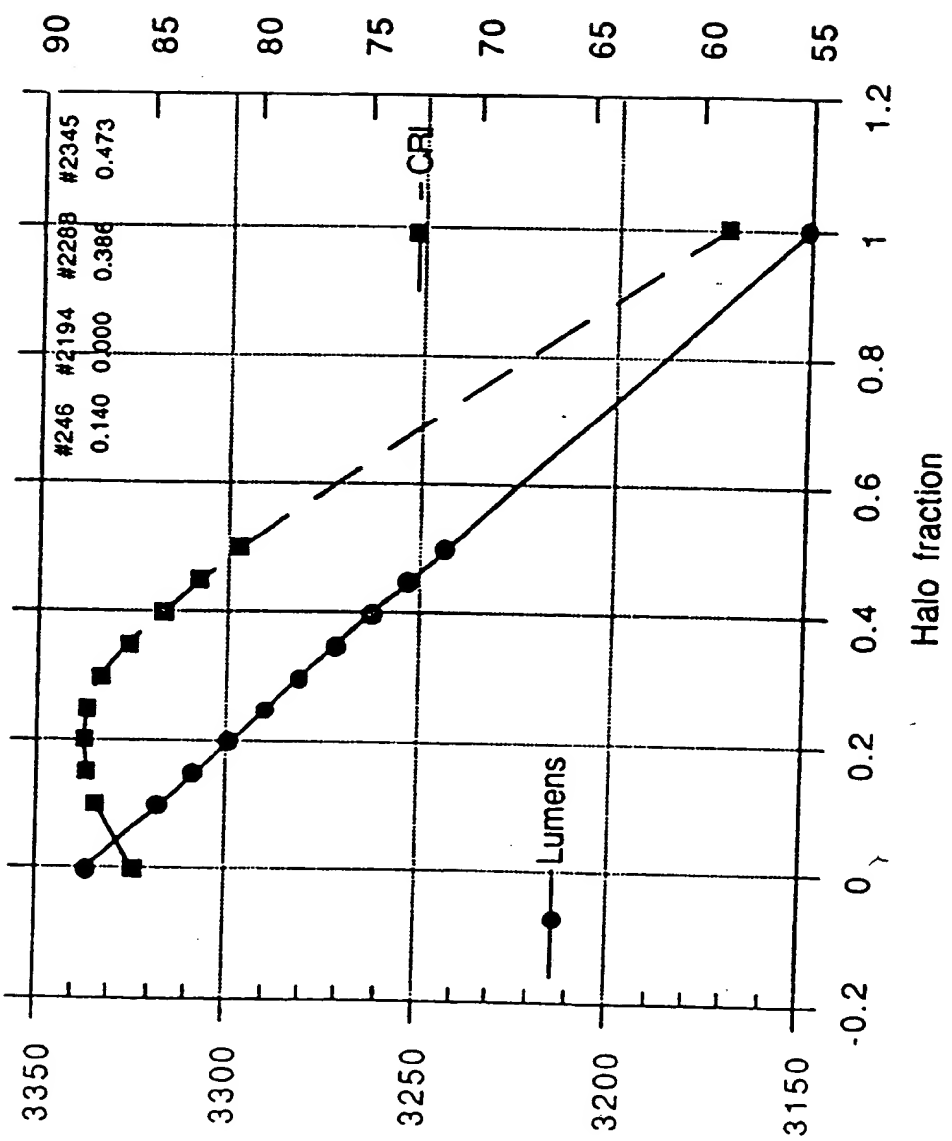

Fig. 12

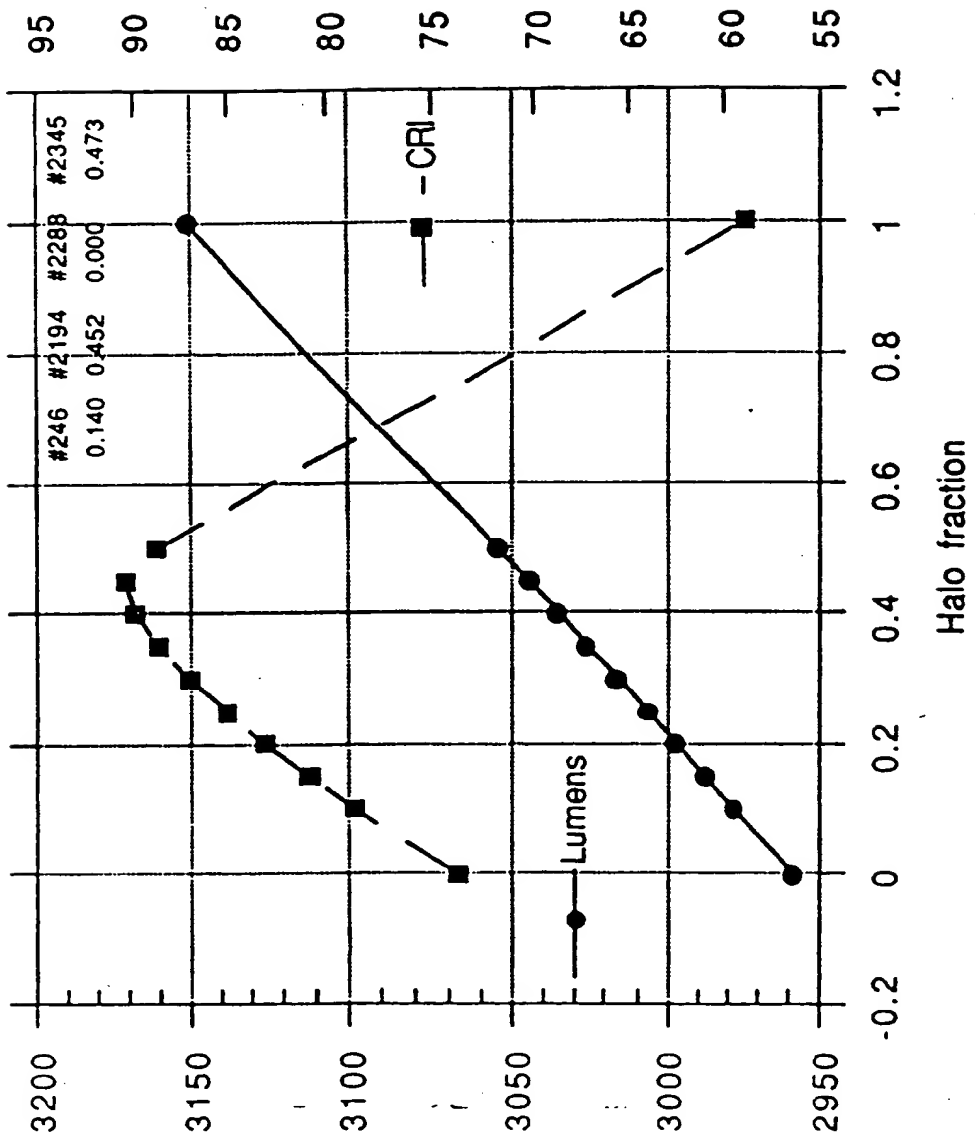

Fig. iii1

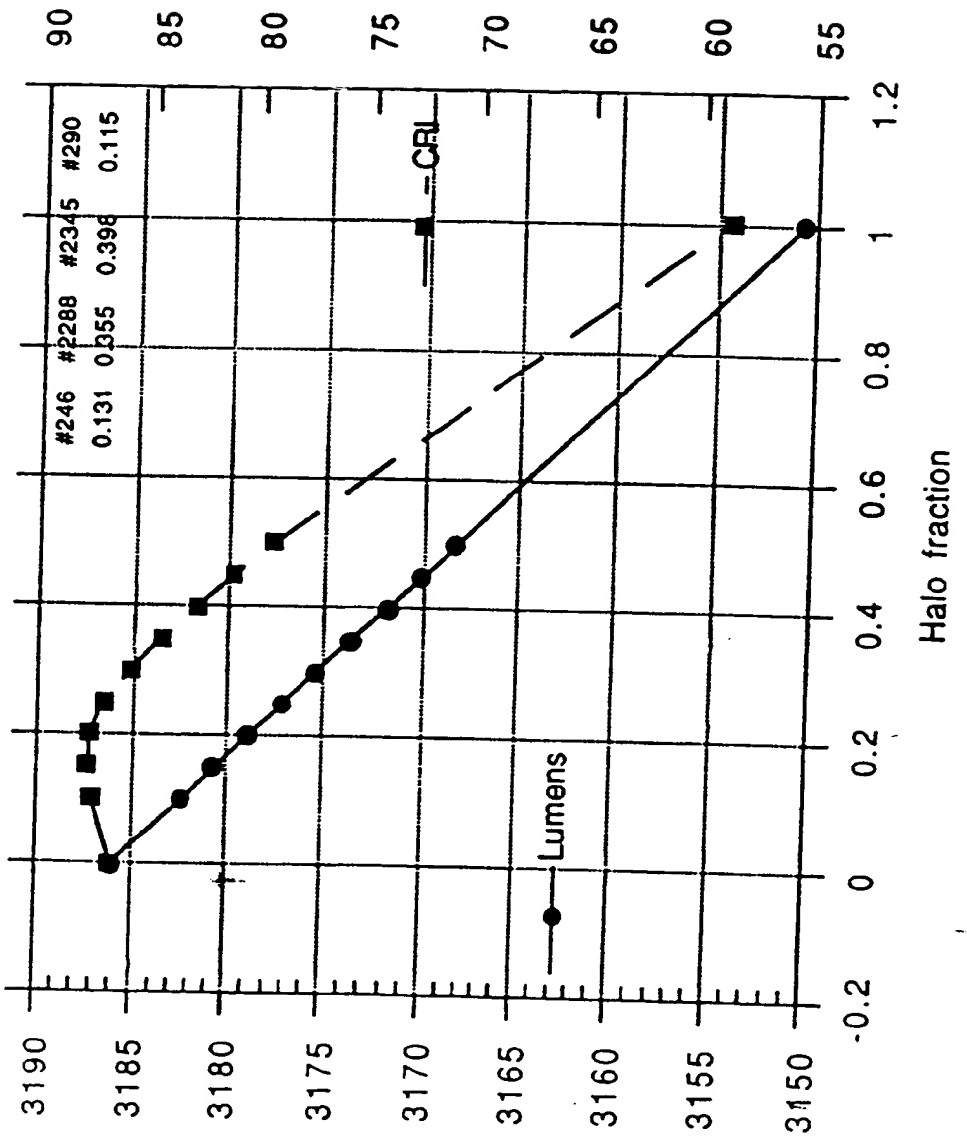

Fig 11

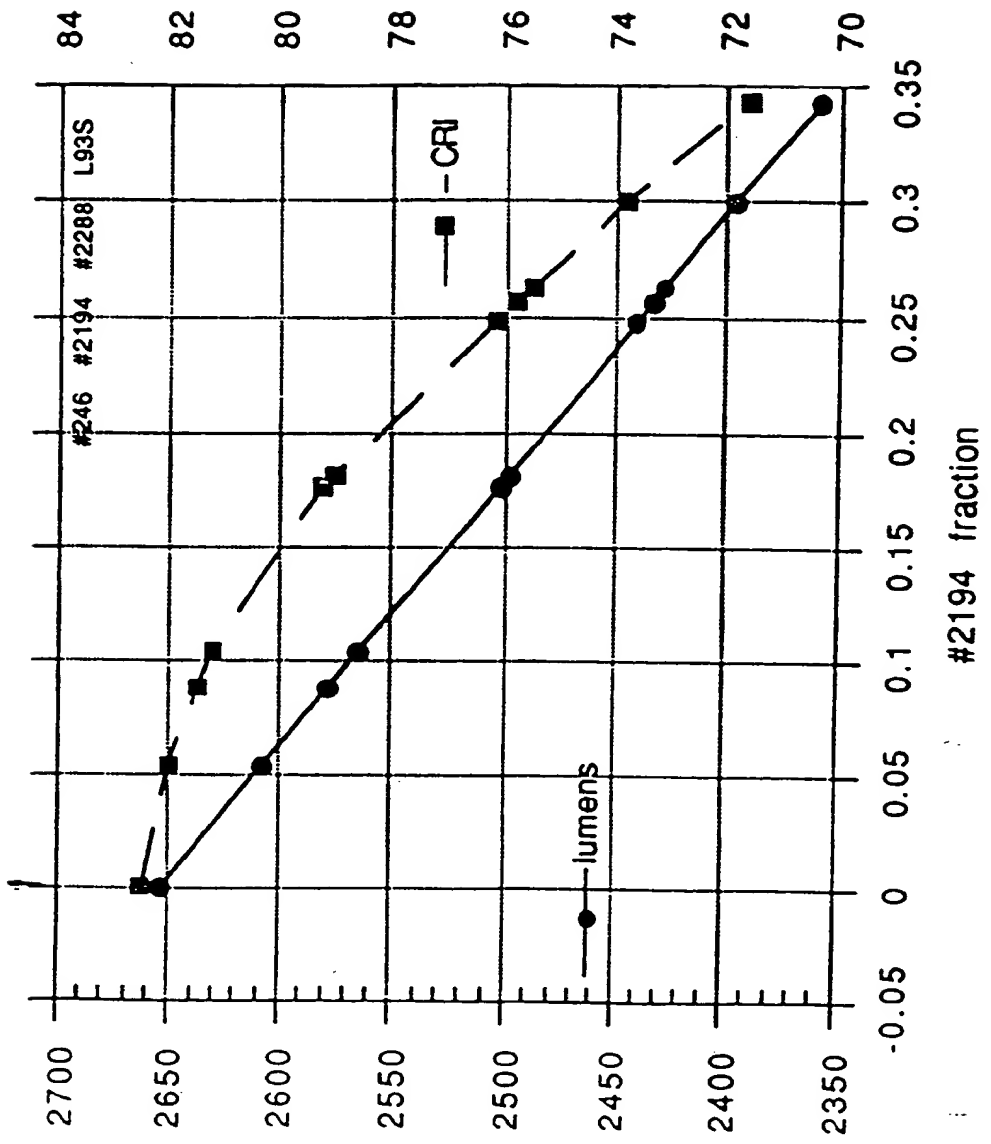

Fig. 12

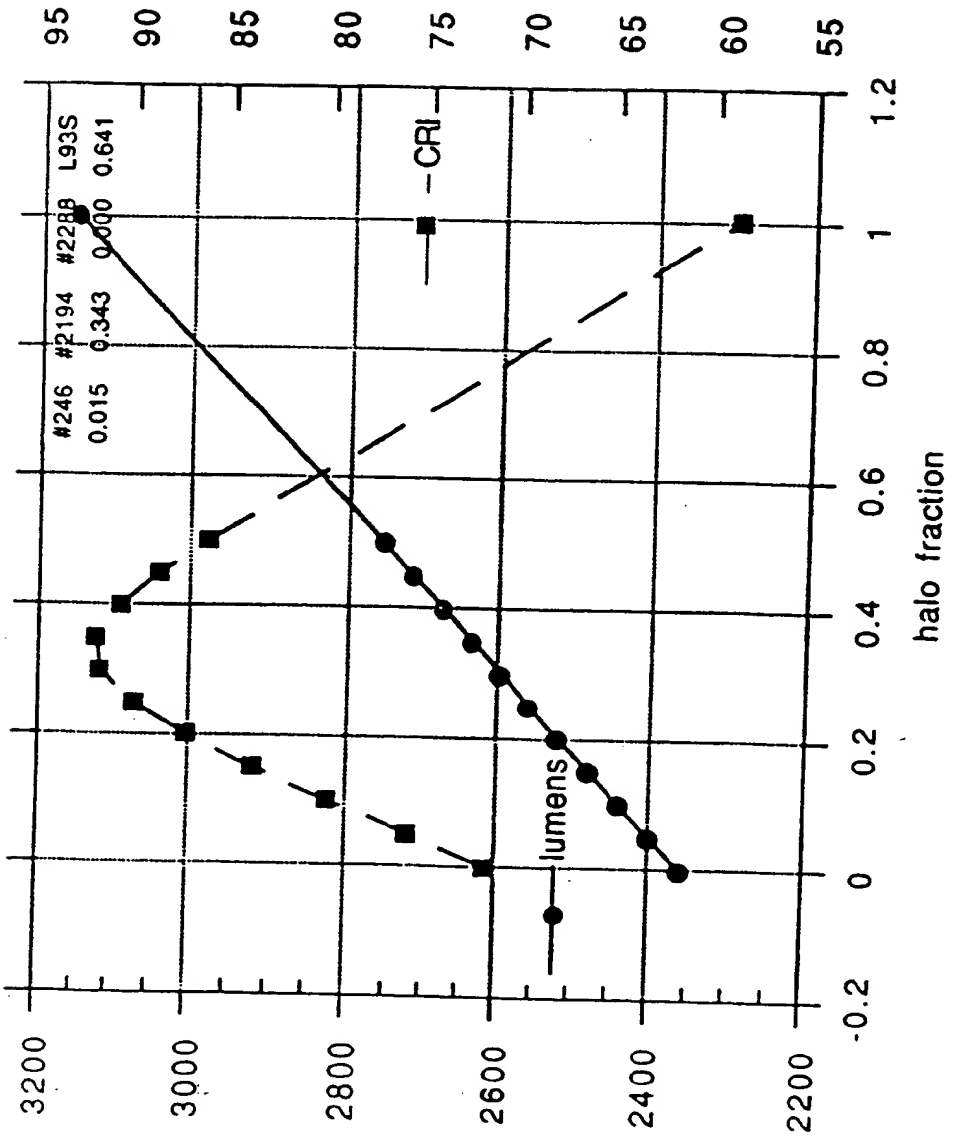

Fig. 1

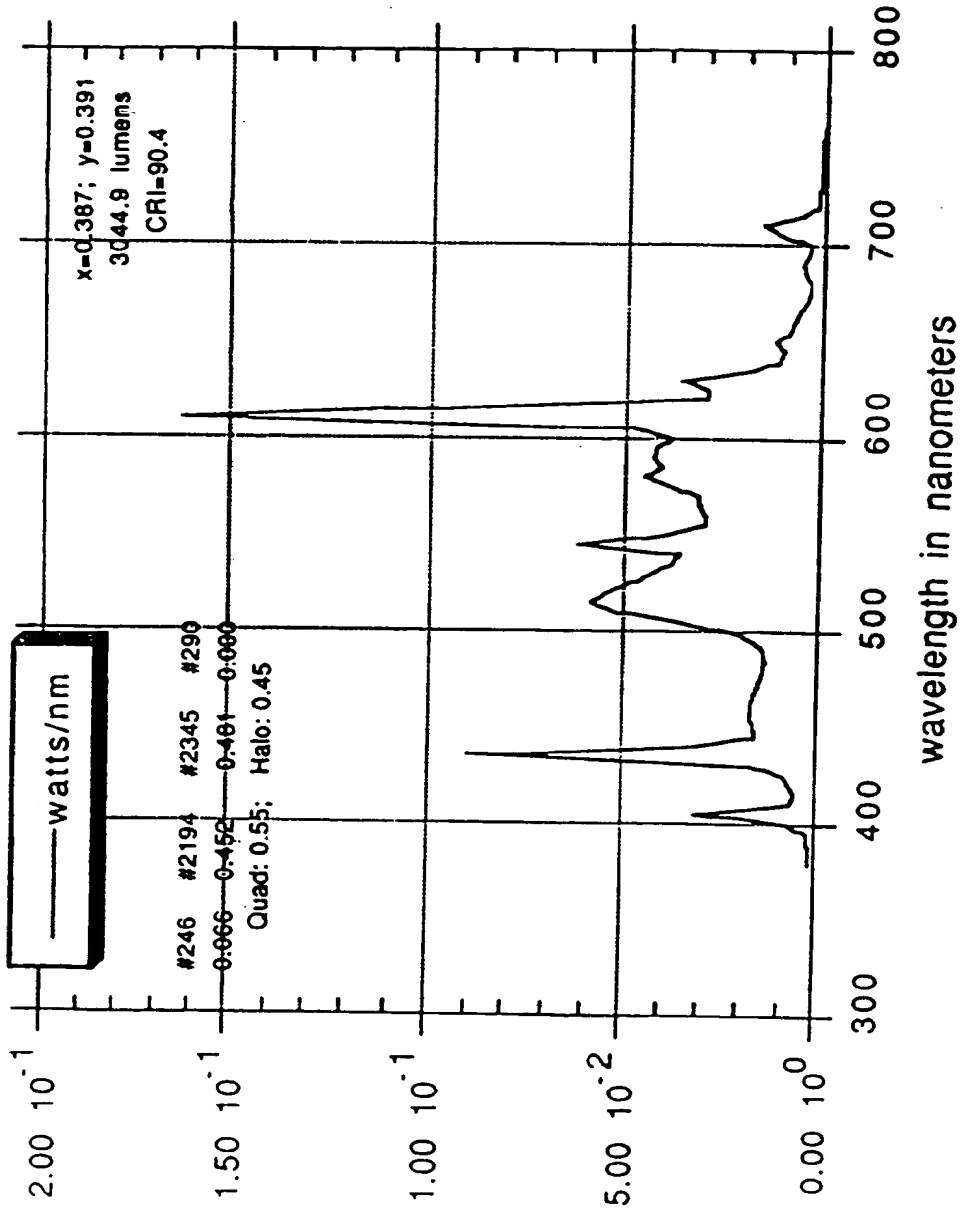

Fig. 1

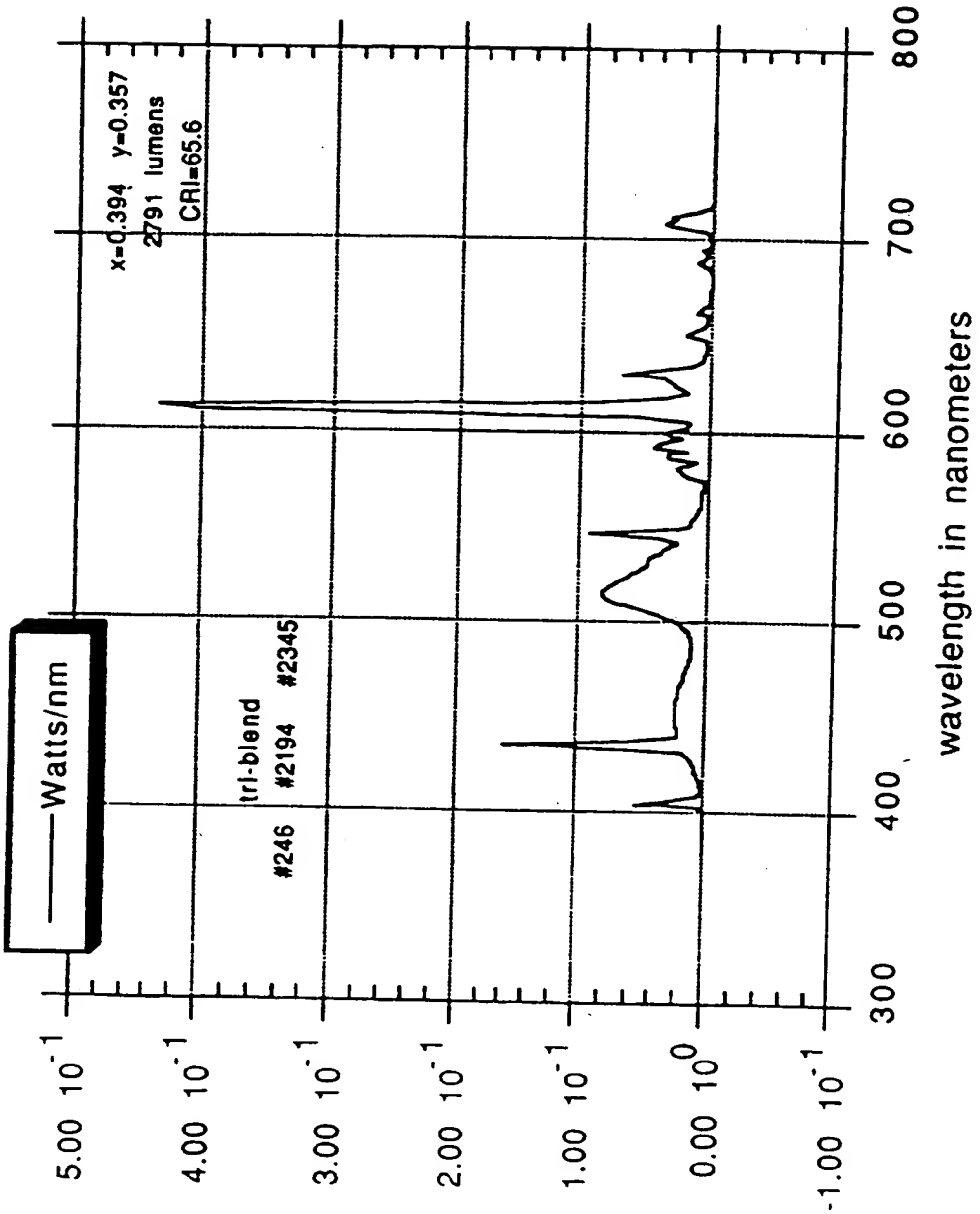

Fig 1 e 2

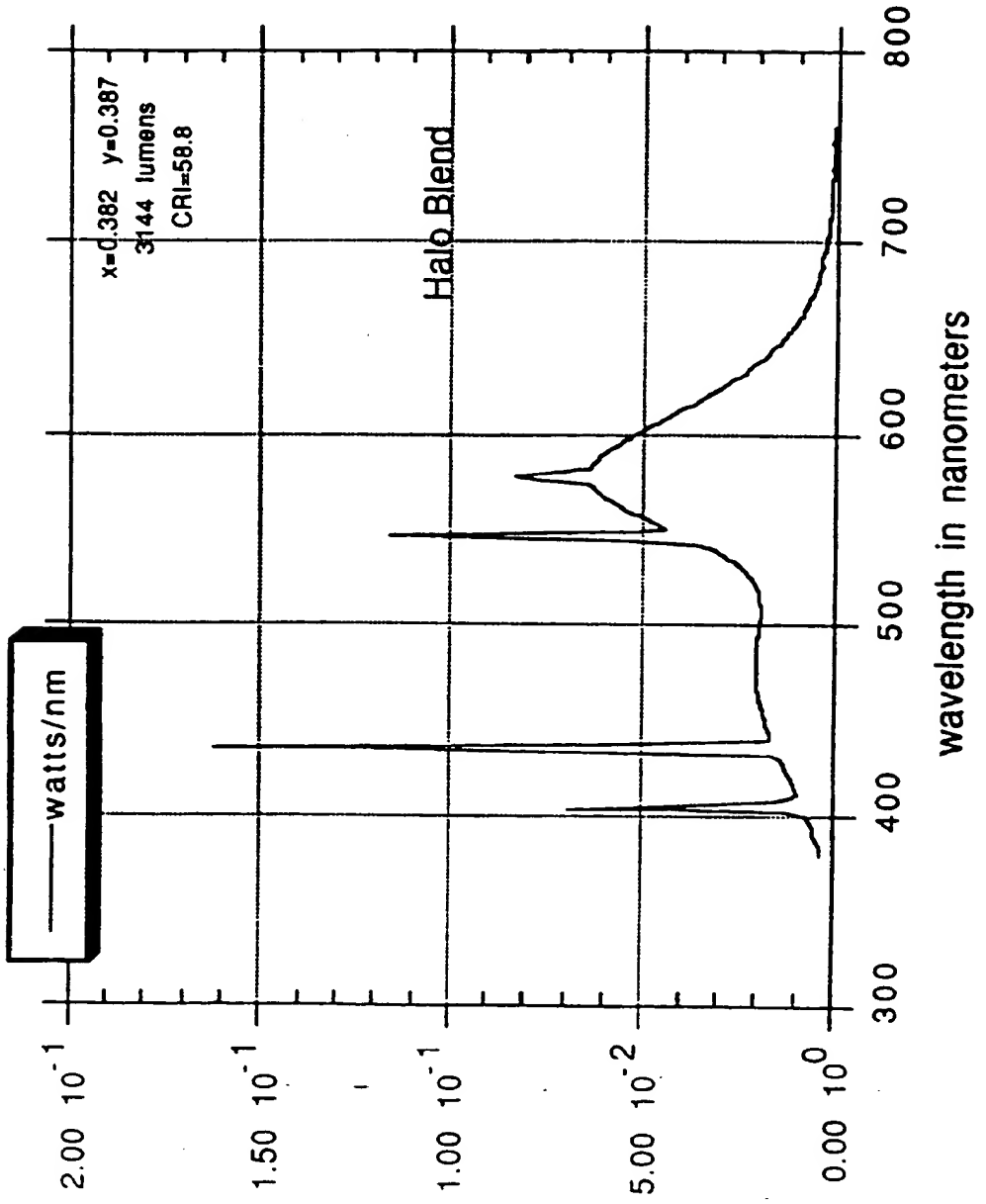

Fig. 3

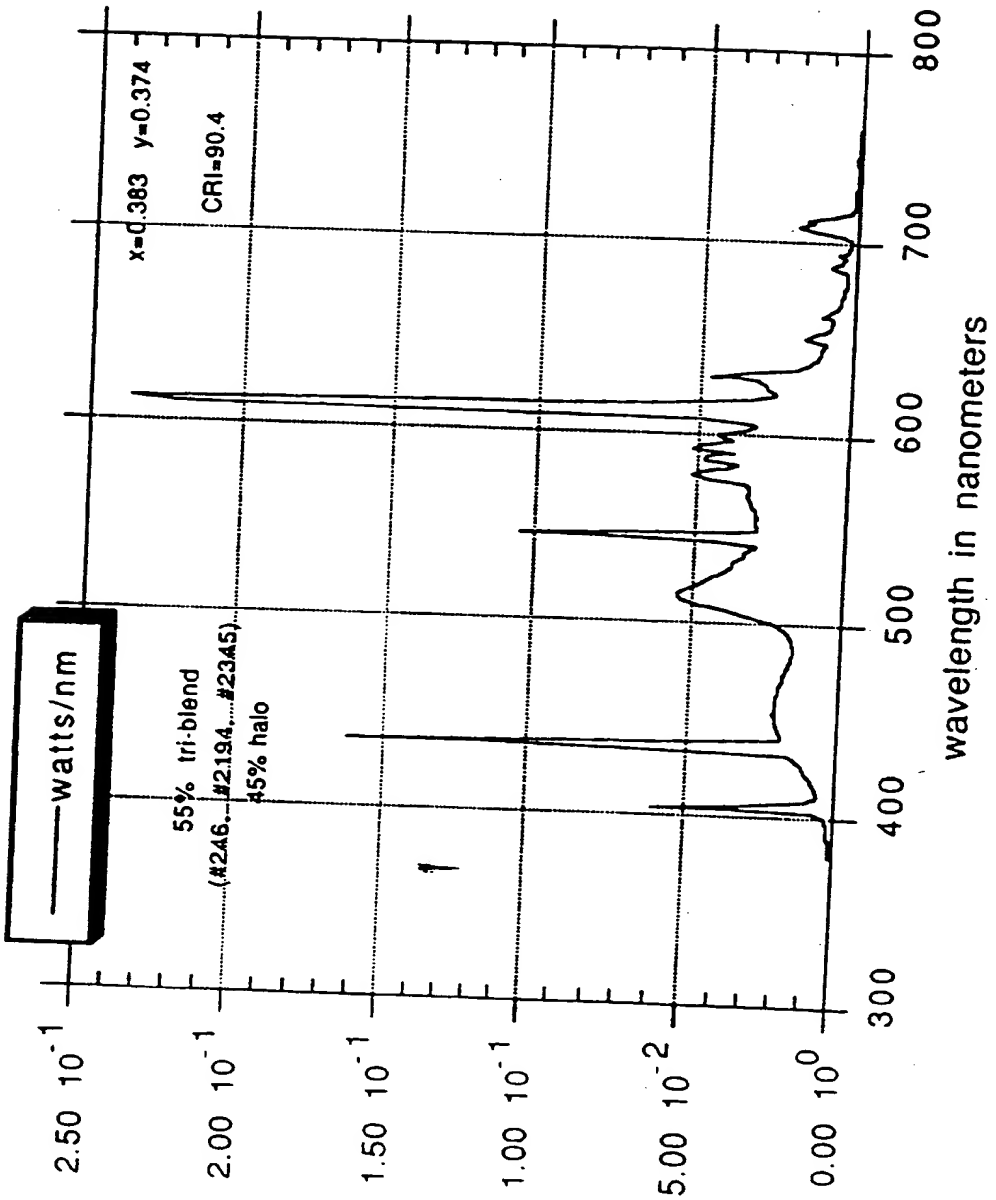

Fig. 61

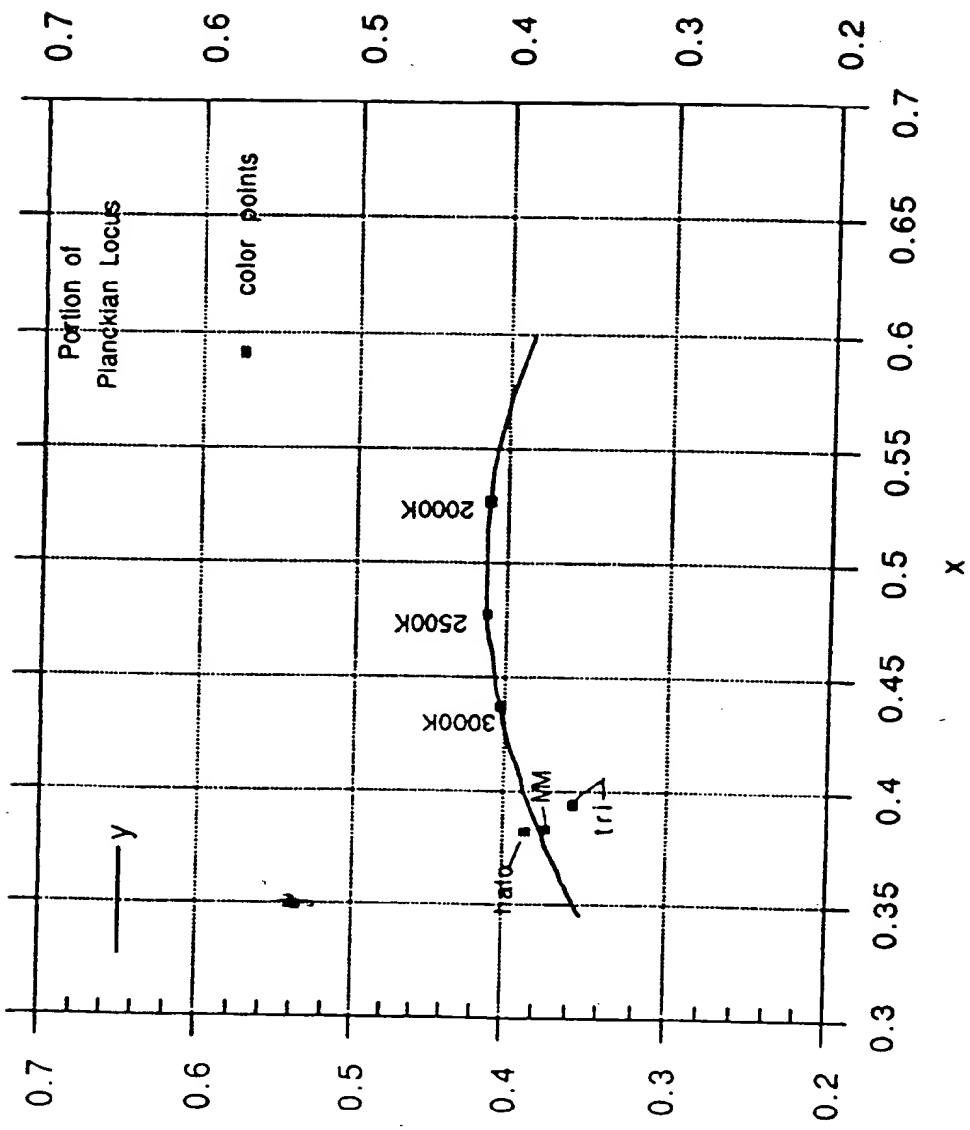

European Patent Office

EUROPEAN SEARCH REPORT

Application Number
EP 93 30 8312

DOCUMENTS CONSIDERED TO BE RELEVANT

Category	Citation of document with indication, where appropriate, of relevant passages	Relevant to claim	CLASSIFICATION OF THE APPLICATION (Int.Cl.5)
A	EP-A-0 257 554 (G.T.E.) * claims 1-57; tables 5-6 *	1-10	H01J61/44 C09K11/72 H01J61/48
A	US-A-4 891 550 (D.NORTHROP & AL) * the whole document *	1-8	
A	PATENT ABSTRACTS OF JAPAN vol. 7, no. 148 (E-184)29 June 1983 & JP-A-58 061 554 (TOKYO SHIBAURA DENKI) 12 April 1983 * abstract *	1-5,7,9	

TECHNICAL FIELDS SEARCHED (Int.Cl.5)
H01J
C09K

The present search report has been drawn up for all claims

Place of search	Date of completion of the search	Examiner
THE HAGUE	17 January 1994	DROUOT, M

CATEGORY OF CITED DOCUMENTS

X : particularly relevant if taken alone
Y : particularly relevant if combined with another document of the same category
A : technological background
O : non-written disclosure
P : intermediate document

T : theory or principle underlying the invention
E : earlier patent document, but published on, or after the filing date
D : document cited in the application
L : document cited for other reasons

& : member of the same patent family, corresponding document

EPO FORM 1503 03.82 (P04C01)